AFRL-IF-RS-TR-2005-37
Final Technical Report
February 2005

PASSIVE MILLIMETER-WAVE IMAGING FOR THE DETECTION OF CONCEALED WEAPONS

Trex Enterprises Corporation

APPROVED FOR PUBLIC RELEASE; DISTRIBUTION UNLIMITED.

AIR FORCE RESEARCH LABORATORY
INFORMATION DIRECTORATE
ROME RESEARCH SITE
ROME, NEW YORK

STINFO FINAL REPORT

This report has been reviewed by the Air Force Research Laboratory, Information Directorate, Public Affairs Office (IFOIPA) and is releasable to the National Technical Information Service (NTIS). At NTIS it will be releasable to the general public, including foreign nations.

AFRL-IF-RS-TR-2005-37 has been reviewed and is approved for publication

APPROVED: /s/
PETER J. COSTIANES
Project Engineer

FOR THE DIRECTOR: /s/
JOSEPH CAMERA, Chief
Information & Intelligence Exploitation Division
Information Directorate

REPORT DOCUMENTATION PAGE

Form Approved
OMB No. 074-0188

1. AGENCY USE ONLY (Leave blank)	2. REPORT DATE	3. REPORT TYPE AND DATES COVERED
	February 2005	**Final** **Jan 03 – Apr 04**

4. TITLE AND SUBTITLE

PASSIVE MILLIMETER-WAVE IMAGING FOR THE DETECTION OF CONCEALED WEAPONS

5. FUNDING NUMBERS

C - F30602-03-C-0054
PE - N/A
PR - CWDP
TA - 03
WU - 01

6. AUTHOR(S)

Chris Martin

7. PERFORMING ORGANIZATION NAME(S) AND ADDRESS(ES)

Trex Enterprises Corporation
10455 Pacific Center Court
San Diego CA 92121-4339

8. PERFORMING ORGANIZATION REPORT NUMBER

N/A

9. SPONSORING / MONITORING AGENCY NAME(S) AND ADDRESS(ES)

AFRL/IFEC
525 Brooks Road
Rome NY 13441-4505

10. SPONSORING / MONITORING AGENCY REPORT NUMBER

AFRL-IF-RS-TR-2005-37

11. SUPPLEMENTARY NOTES

AFRL Project Engineer: Peter J. Costianes/IFEC/(315) 330-4030 Peter.Costianes@rl.af.mil

12a. DISTRIBUTION / AVAILABILITY STATEMENT

APPROVED FOR PUBLIC RELEASE; DISTRIBUTION UNLIMITED.

12b. DISTRIBUTION CODE

13. ABSTRACT ***(Maximum 200 Words)***

The passive millimeter-wave camera (PMC) is a second generation millimeter-wave (MMW) imaging system delivered to the National Institute of Justice for evaluation as a concealed weapons detection system. The PMC uses an unusual pupil-plane architecture as opposed to the focal plane architecture common in other MMW systems. A frequency-scanned phased-array antenna paired with a number of quasi-optical MMW processing boards allows the system to create a wide field-of-view video rate image while using a relatively small number of MMW amplifiers. The system also occupies a small volume compared to focal-plane based systems. This paper details the components that make up the imager, including the flat-panel antenna, MMW amplifiers, processor boards, diode detectors, digital read-out circuits, and MMW transitions. The paper also describes the construction of these devices and the integration of the PMC system. Integration includes phasing the system front-end, setting back-end power levels, and building and testing frequency processor board arrays. The PMC imager has problems with feedback into the antenna and calibration drift, but the system was tested for performance, including angular resolution and temperature sensitivity. The test procedures are discussed here and the test results are attached to the document.

14. SUBJECT TERMS

Millimeter Wave, Phased Array Antenna, Imaging, Rotman Lenses, Low Noise Amplifiers

15. NUMBER OF PAGES 68

16. PRICE CODE

17. SECURITY CLASSIFICATION OF REPORT	18. SECURITY CLASSIFICATION OF THIS PAGE	19. SECURITY CLASSIFICATION OF ABSTRACT	20. LIMITATION OF ABSTRACT
UNCLASSIFIED	UNCLASSIFIED	UNCLASSIFIED	UL

Table of Contents

List of Figures

Introduction

This final report describes the results of Contract Number F30602-03-C-0054 between Trex Enterprises Corporation and the U.S. Air Force Research Laboratory (AFRL), Rome Research Site. The objective of the program, a follow-on to a previous contract, DAAL01-94-C-0100, was to fabricate, test, demonstrate, and deliver a second generation passive millimeter-wave camera (PMC) suitable for real-time concealed weapons detection. Funding for these programs came from the National Institute of Justice (NIJ), Washington, DC.

The system known as PMC-2 (Figure 1) uses Trex Enterprises Corporation's (Trex) patented flat panel antenna and millimeter-wave signal processors to enable a 30 by 20 degree instantaneous field of view true real time (30 Hz) sensor to be built in a portable 2 foot square by 10 inch deep package.

The millimeter-wave (MMW) portion of the electromagnetic spectrum, specifically 75 to 93 GHz, is chosen as it offers a good balance between clothing penetration as well as resolution and therefore allows compact, practical sized systems suitable for law enforcement to be built. By measuring only the natural thermal emissions from living beings and inanimate objects, passive millimeter-wave imaging is intrinsically safe and suitable for imaging people.

The PMC-2 imager uses a novel frequency scanned phased array flat panel antenna coupled to MMW low noise amplifiers (LNAs), to produce enough signal to allow a two-dimensional MMW Rotman lens (comprised of one phase processor and 192 frequency processors), to perform the Fourier transform that is needed to go from the antenna (pupil plane) to the image plane. Custom detector diodes and A/D chips are then used to detect and digitize the image plane MMW signal. The digitized signal is then fed to a high performance PC for processing and display.

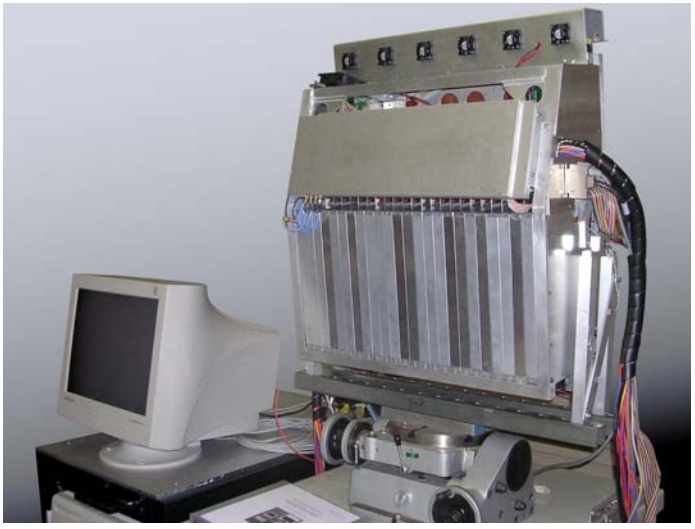

Figure 1. PMC-2 imaging sensor.

Concept of Operation

The Passive Microwave Camera, or PMC, is a real-time imaging radiometer. It creates imagery from the blackbody radiation in the W-band between 75.5 to 93.5 GHz emitted

or reflected by targets within the field of view. The received power level is displayed to the user as intensity at a 30 Hz frame rate. The wavelength of the imaged energy (3-4 mm) allows it to pass through obscurants which scatter or absorb infrared and visible light. As a result, the PMC can image through fog, smoke, and steam, and also image concealed objects under people's clothing or behind some light materials.

The most common architecture for millimeter-wave imaging systems is the focal plane array. An array of amplifiers or detectors, each one representing a pixel in the image, has incoming microwave energy focused on it by a lens or reflector. The lens or reflector is necessarily removed from the detector array by a path length equal to its focal length, forcing the system to have a large volume for a large aperture. The PMC instead uses pupil-plane architecture. In this architecture, the microwave energy is captured at the aperture before being focused. After amplification, the energy is processed to determine from what angle the energy arrived at the aperture. The PMC uses both phase and frequency processing to guide the energy into individual detector diodes. The frequency-scanned antenna is selectively sensitive to various frequencies depending upon angle of incidence in elevation. Amplifiers fed by the antenna act as elements of a phased array to determine the angle of incidence in azimuth. Novel phase and frequency processors then use the phase and frequency information of the signals to focus the energy on individual detector diodes. The energy level recorded at each diode is displayed as a pixel in the image. The pupil plane architecture allows for a lower volume system because it eliminates the space between an aperture and detector array. It also allows the system to use fewer low noise amplifiers to produce a large number of image pixels.

The second generation PMC consists of the following major subsystems: the flat panel antenna, the front-end switches and octopak amplifiers, the phase processor, the back-end amplifiers, the frequency processor and detector diodes, the read-out chips and interface board, and the computer. The block diagram of these components is laid out in Figure 2.

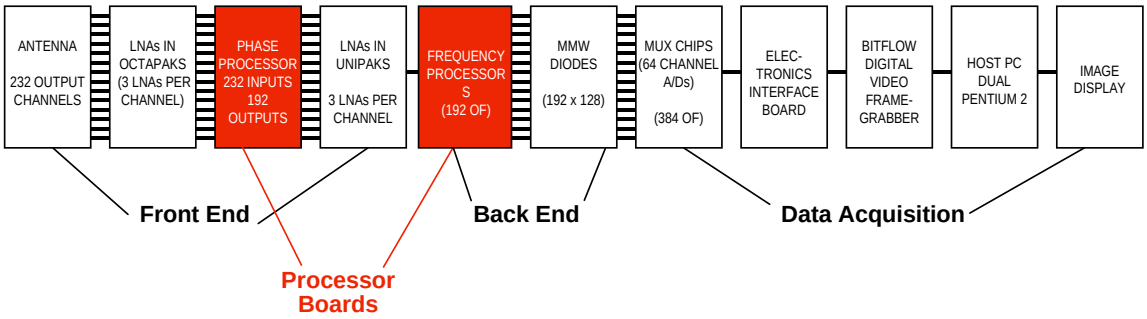

Figure 2: Block diagram layout of PMC major components

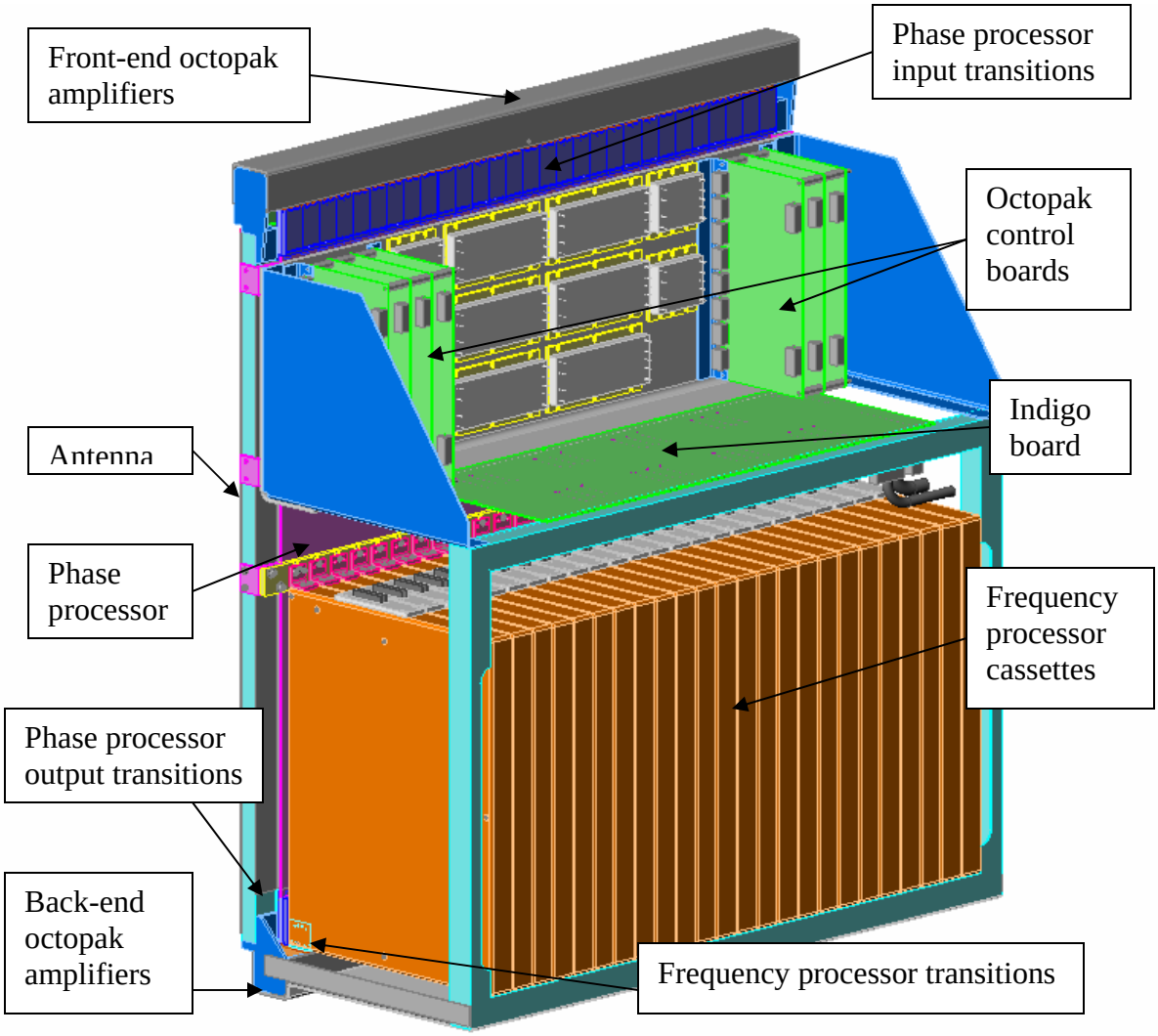

Figure 3: Mechanical drawing of passive microwave camera sensor

PMC Photos

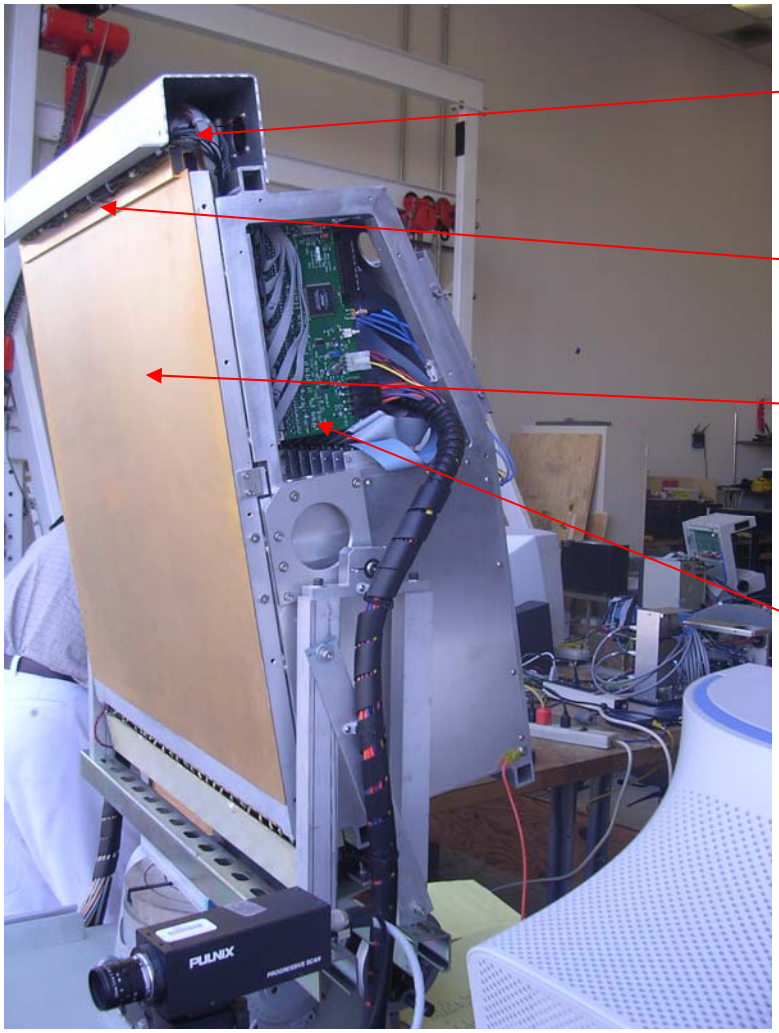

Front-end octopak amplifiers

Antenna transition

Antenna

Octopak control boards

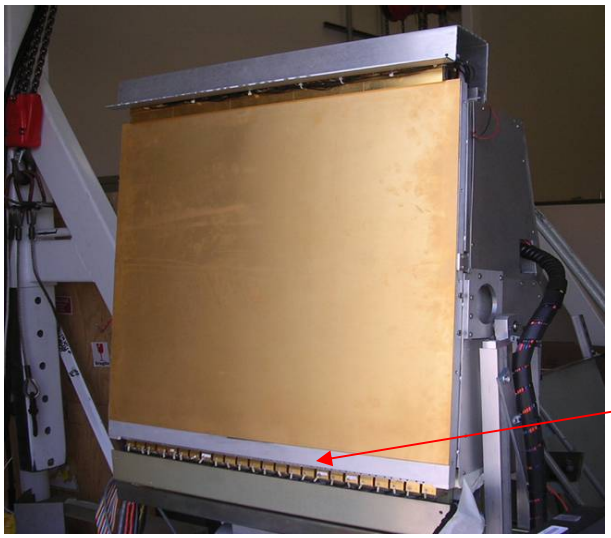

Back-end octopak amplifiers

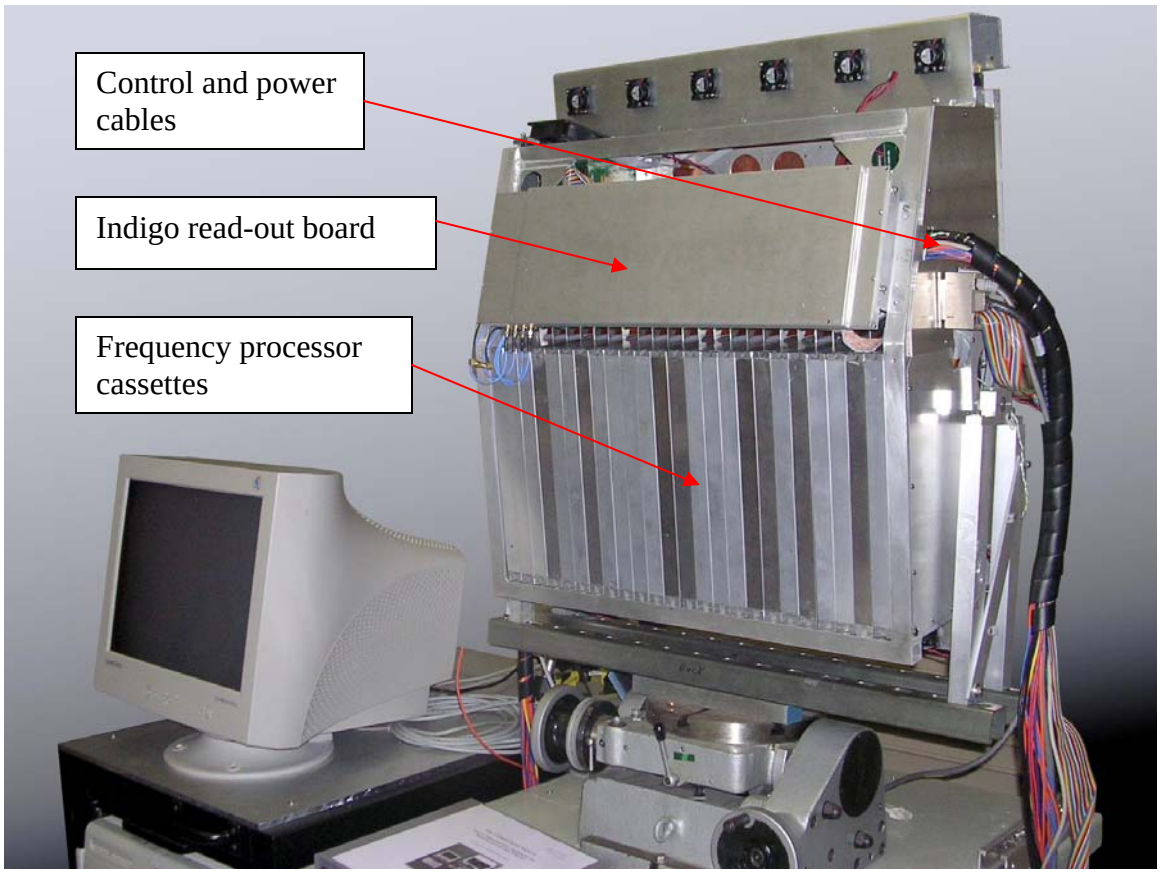

Components

Antenna

The PMC's flat panel antenna is composed of a low loss 30 mil thickness polyethylene dielectric (ε=2.2) sandwiched between two layers of electro-deposited copper (Fig. 4). This structure acts as a parallel plate waveguide, which supports TEM transmission. The antenna has an active area of 23" (V) by 24" (H) where one of the copper planes is perforated by a 298x400 array of slots. The regularly spaced slots act to couple free space energy from the outside world to the modes supported by the antenna. The degree of coupling can be tuned by adjusting the slot width. By choosing a slot spacing close to the wavelength in dielectric of the desired signals, the antenna becomes frequency selective;

Figure 4: Flat panel dielectric antenna.

i.e. for a specific angle of incidence on the antenna relative to the slot spacing, only one frequency will constructively interfere inside the antenna. In this way, the source angle of the incoming radiation to the antenna can be determined by its frequency. The slot orientation determines the direction of travel for coupled energy, perpendicular to the long slot edge.

The second generation PMC has an antenna with 78-mil slot spacing resulting in a frequency scan of 23.25 degrees from 75.5 to 93.5 GHz (Figure 5). The beamwidth of the antenna in the frequency scanned direction is close to the diffraction limited performance of a 2 foot aperture. Frequency discrimination is 330 MHz based on the delay time from antenna top to bottom. The slot width was chosen as 32 mils to maximize energy coupling to the antenna in each slot while still using the entire aperture. The measured loss of this antenna averages 4.5 dB, which is about 1 dB more than predicted, perhaps indicating that a higher coupling coefficient was needed. This antenna is inexpensive and easy to produce because the coupling slots are etched photolithographically. It is also light, weighing less than 15 lbs. including the Teklam baseplate and antenna transition.

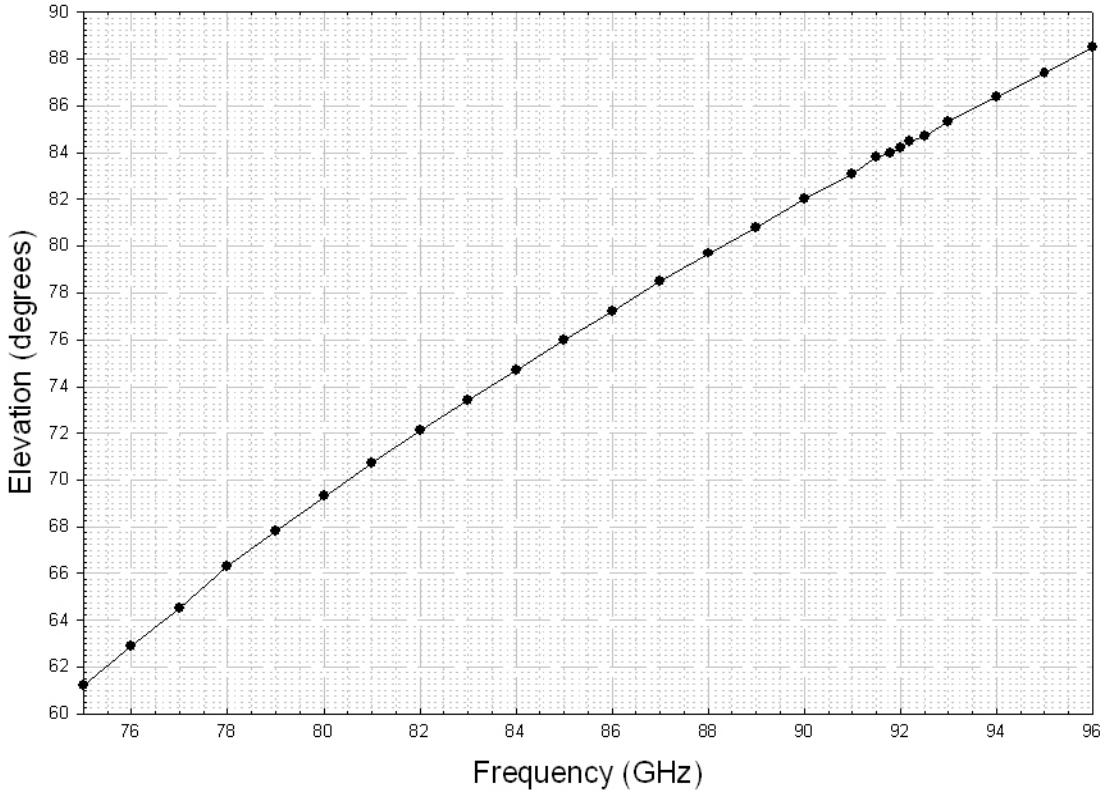

Figure 5: Antenna beam angle vs. frequency

Octopaks

The octopak amplifier units consist of eight MMW amplifier channels integrated into a single housing. Each channel also contains a front-end switch and a band-pass filter. The block diagram for a single channel is shown in Figure 6.

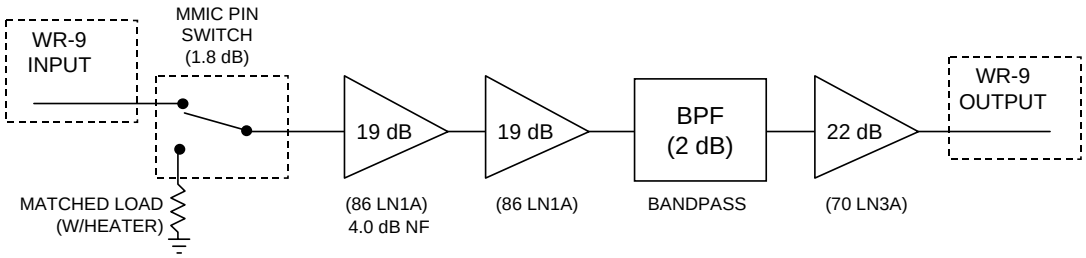

Figure 6: Block diagram of an amplifier channel in an octopak

Amplification is provided by three InP MMIC amplifiers produced by HRL of Malibu, CA. HRL produced two designs: the 86LN1A and 70LN3A, each using HEMT device technology. The 86LN1A had a somewhat lower noise figure and is used as the first and second stages. The 70LNA3 has a somewhat higher gain and compression point and is used as the final stage. Between the input to the octopak and the first amplifier is a MMIC PIN switch. Between the second and third stage is a bandpass filter.

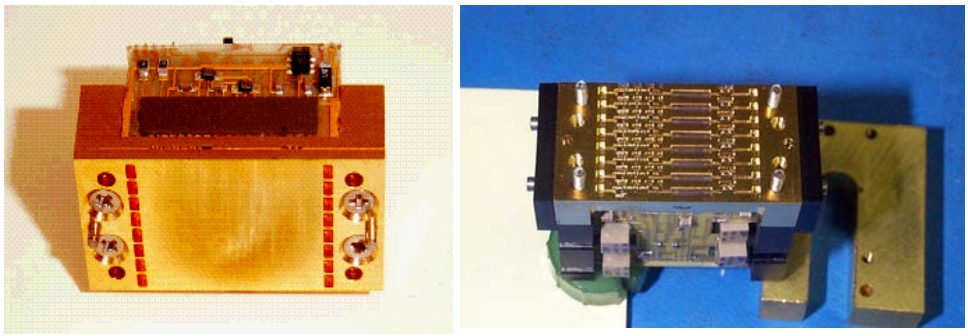

Figure 7: Octopak and bottom cover plate with input and output waveguides, octopak with bottom cover plate removed to expose amplifier channels

The amplifiers, switch, and filter are connected through microstrip transmission lines on Duroid, which are wire bonded to each module (Figure 8). The input and outputs to the octopak package are WR-9 waveguide which transition to microstrip through a waveguide probe matched transition. The waveguide package itself is 0.825" wide by 1.5" long. This package size allows us to densely pack 232 waveguide inputs into a 24" linear array.

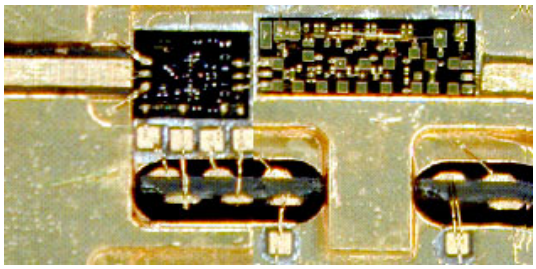

Figure 8: Close up of the PIN switch and first MMIC stage in one octopak channel. The input microstrip line is on the left, output microstrip line on the right, and PIN switch control lines at the bottom.

The octopak amplifiers were originally designed to operate from 77 GHz to 95 GHz. Initial testing showed that the MMIC amplifiers rolled off in response at the high end, so the decision was made to operate the PMC from 75.5 to 93.5 GHz. The gain of each module varies from 50-55 dB, and the noise figure of the packaged unit is 7-8 dB.

PIN Switch

A GaAs MMIC PIN switch manufactured by M/A-Com is located at the input to the first amplifier. The output line of the switch is the base of a 'Y'-junction where either arm of the Y leads to a PIN diode through a quarter-wave transmission line. When either diode is conducting, that path appears as a quarter-wave short to the output. When open, the path appears as a 50 ohm transmission line. At any time, the bias applied to the diodes is such that one diode is shorted while another is open. To change the switch state, the bias on the diodes is reversed. In one switch state, the switch appears as a direct transmission line to the switch input. In the other switch state, the switch output is terminated in a 50-ohm resistive load. The PIN switch serves as the Dicke switch for the imaging radiometer. In operation, the PIN switch is switched at 3.84 kHz (a 1.92 kHz cycle) between the switch input and load. The power values obtained at these two states are differenced at the MUX chip detector circuit.

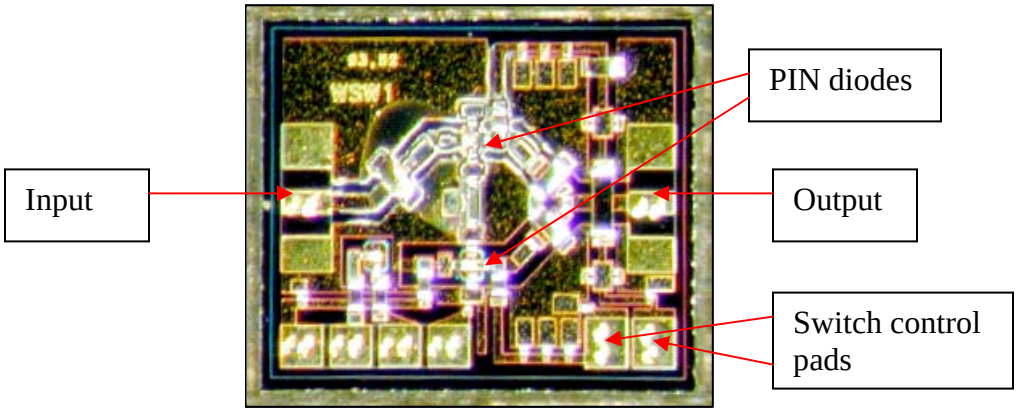

Figure 9: MMIC PIN switch.

The 50-ohm load in the PIN switch can be is used as an ambient temperature reference. The load can also be heated with a 30 mA current to provide a second temperature reference point approximately 30-50 K above ambient. This heated load was designed to serve as a 2-point calibration reference for the system. In this mode, the heater was designed to be switched on and off at 1.92 kHz with the power difference between the two states measured at the MUX chip detector circuit. The magnitude of the difference would be used to track changes in the gain of the system amplifiers. The 2-point calibration scheme was never implemented in PMC-2 due to difficulties with feedback and problems implementing the gain correction algorithm.

M/A-Com made two separate runs of PIN switches for the PMC-2 octopaks. The first run of PIN switches had a loss of about 2 dB, but also had structural problems. The backside metallization was peeling off the chips and the air bridges on the chip face were

easily damaged during handling. A second run of PIN switches had better adhering metallization and added a BCB dielectric layer across the face of the chip to protect the components. However, these PIN switches had a loss which averaged 4 dB, 2 dB greater than designed. M/A-Com later attributed this loss to a bad GaAs substrate that had a large number of dissociation faults. The first run of PIN switches was used in the first fifty of the octopaks produced while the second run was used in the remainder.

Octopak Power and Control

The octopak package includes all the power distribution and control signal electronics. The power and control signals from the octopak control boards reach the octopak on a 16-pin connector resting on a distribution board. This board contains switches for the PIN switch and heater circuits and distributes the bias voltages to eight bias boards, which sit parallel to one another above each octopak channel and perpendicular to the distribution board. The bias boards have a voltage regulator for the drain voltages and resistor networks for the other signals to control the current and voltage to the MMICs. Bond wires transfer the currents from the edges of the bias boards to the MMICs. The case of the octopak serves as a common ground for all chips.

Figure 10 shows the layout of the traces and pin functions on the distribution board. Each 'Q' indicates a FET placement, while the 'C' indicates a bypass capacitor. The position of the bias board for each channel is shown to the right of the diagram. The destination of the voltages distributed to the bias boards by the vertical traces are labeled below the diagram. Wire jumpers bridge gaps in the traces to create a bus that runs across the board for these voltages. The only exception to this is the drain current, which draws enough current to require separate lines for each channel.

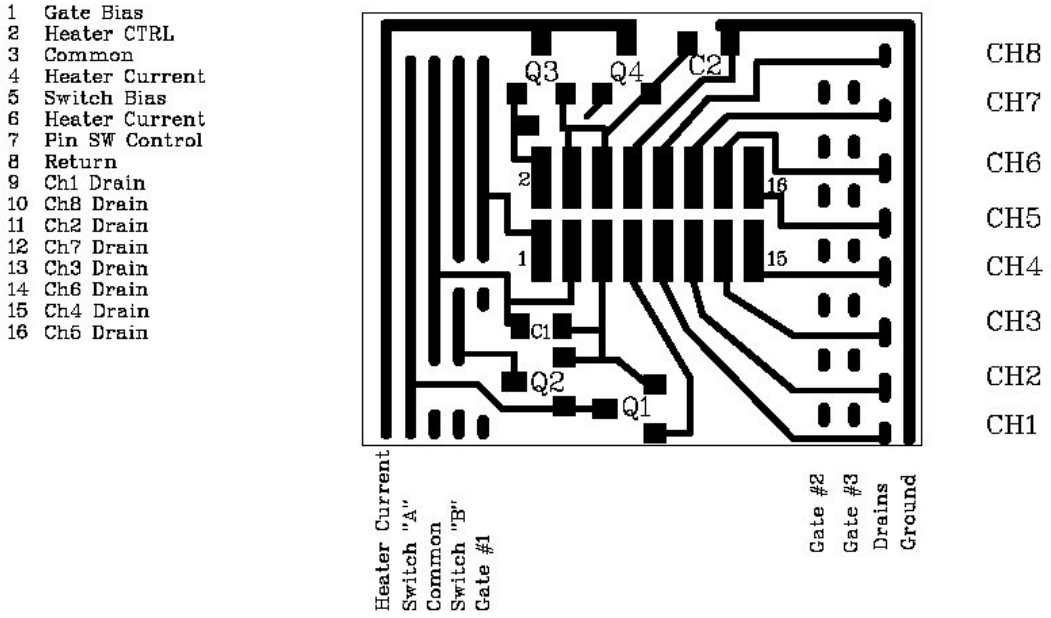

Figure 10: Octopak distribution board layout and pin functions

The voltage and functions of each pin on the 16-pin connector are detailed here. The gate bias is nominally -1 V at the connector and is distributed to the gates of each of the three MMIC amplifiers by the bias boards. However, each octopak amplifier has its gain profile individually tuned by tuning the gate voltage. A resistor network on the distribution board sets some of these gate voltages, especially on gate #2, to a value between -1 V and 0 V before being fed to the bias boards. The individual bias boards have a voltage divider which further raises the gate voltage before feeding the MMIC gates. Raising the gate voltage toward 0 V will generally raise the gain of the amplifier. The heater control line is a TTL signal which controls the two FETs on the heater current line. When the TTL signal is low, the FETs are turned on and the heater current flows to the load. The heater current lines are biased to 3.3 V, and when the FETs are activated the current flows through a 50 ohm resistor on each bias board, and then through the 50 ohm load itself. The total current draw is about 250 mA, which is why there are two lines used for this current. The switch bias line is set at 5V and runs to each of two FETs which are tied to the PIN diodes MMIC switch. The pin switch control is a TTL signal which controls the first of these FETs. The second FET is controlled by the output of the first FET. Because a low signal turns the FET on, only one FET is ever on at one time. This effect provides the 5 V to either the switch 'A' control line or switch 'B' control line. When the PIN switch control line is low, the switch is set to see the input, or the PMC antenna. When the PIN switch control line is high, the switch is set to see the resistive load. The 'A' and 'B' switch control lines are connected to the switch through 200 ohm resistors on the bias boards. The common and return lines are both ground lines, connected to the octopak case. The drain lines are biased at 3.3V and provide power to the MMIC amplifiers. Drain currents for each amplifier channel vary from, 80 mA to 135 mA. Each of the bias boards contains a voltage regulator to drop this voltage down to 1.7 V before it is passed through protection diodes to each of the MMIC drains.

Octopak Control Boards

All control and voltage signals for the octopak are supplied by an octopak control board. Each octopak control board serves eight octopaks and there are a total of seven boards in the PMC-2 system. The control board receives power from both a 3V connection and a +/- 5V connection. In addition to the 16-pin control cables for the octopaks, a ground connection on the board can be connected to the octopak case. This provides a heavier gauge ground wire to handle the high drain and heater currents. In practice, all ground connections are not used because the cases of all octopaks are tied together through the PMC frame.

The octopak control board produces the -1V gate voltage, the exact level of which is set with the potentiometer. The 3.3V heater and drain voltages are distributed by this board. The drain voltage for each octopak channel passes through its own FET, which is controlled by the Altera EPLD (erasable programmable logic device). This enables the user to turn on and off the drain voltage to any channel, effectively turning off the amplifier. The control is exercised with a 37-pin computer control cable daisy chained to each octopak control board and tied to the EPLDs. A four-bit DIP switch is used to set the address of each octopak control board so the computer can select between them. Addresses 0-3 are used for octopak control boards controlling front-end octopaks while

addresses 4-6 are used for the back-end octopak control boards. The heater and PIN switch TTL control signals are generated by the octopak control board EPLD. They can be set by computer or they can be controlled by an external signal input to the board on an SMA connector. In normal use, the front end switching signals are controlled by the 1.92 kHz clock signal generated on the Indigo ROIC board and fed to the switch signal input on SMA cables. If the control board ever enters a state where it is unresponsive to computer commands, a chip reset switch on the board restarts the power to the EPLD.

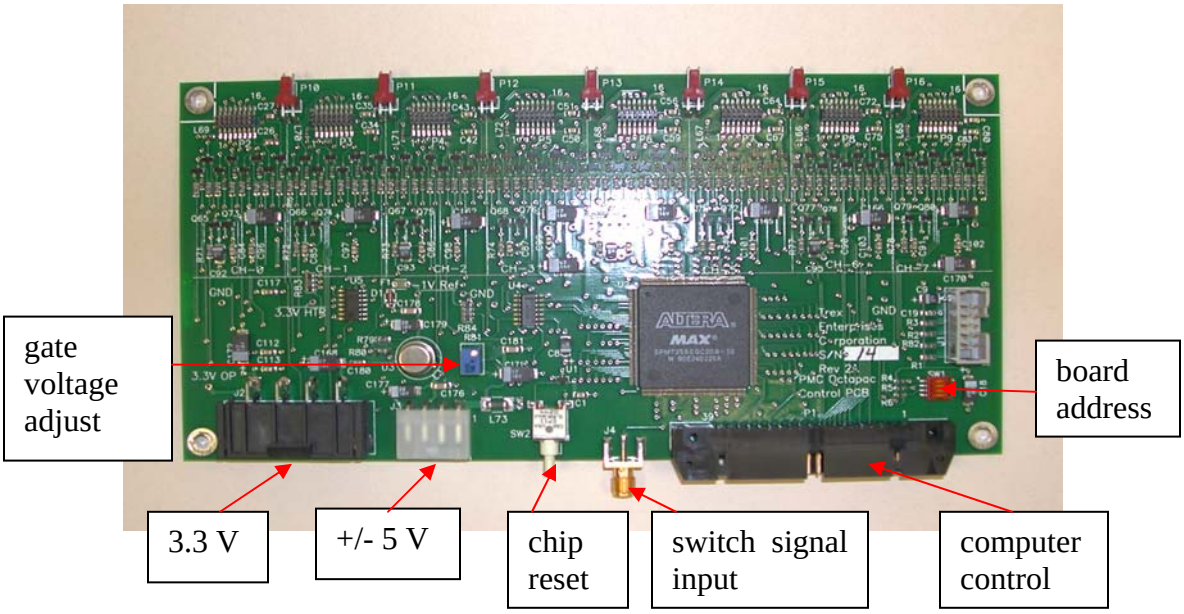

Figure 11: Octopak control board

Phase Processor Board

The phase processor serves the function of sorting the signals received by the phased array into separate channels based upon their angle of incidence on the antenna in the plane of the array. The relative phase of the signals across the amplifier array is determined by this angle of incidence, and the processor uses this phase differential to steer the beams to a particular output port. The operation of the processor is similar to that of a Rotman lens, but the PMC phase processor has had its lens shape slightly altered from the equations describing a Rotman to take advantage of the larger phase tolerance of a passive system and to minimize the processor's size. The processing between the inputs and outputs occurs in a two-dimensional microwave lens. The signals from each antenna element travel to this lens on equal length transmission lines which run in a bootlace pattern and enter the lens on evenly spaced horns on an arc. The microwave lens performs a 1-D spatial Fourier transform on the input signals in an analog to the 2-D transform performed by the lens in a focal plane array. The signals are carried out of the lens by 192 evenly spaced output transmission lines (Figure 12).

Trex Enterprises went through an extensive search for low loss materials appropriate for a phase processor. Polypropylene, $\varepsilon = 2.2$, was chosen as a dielectric for its availability

and low loss tangent, $\sigma = 0.006$. Polypropylene was available in a variety of sizes with copper cladding. When fashioning high frequency circuits on this material, we found that the loss in the circuits was influenced as much by the smoothness of the copper as the loss tangent of the dielectric. Rough copper interfaces with the dielectric force the current to travel an effectively longer path when the skin depth of the current approaches the roughness of the copper surface. The longer path adds to the resistive losses that attenuate a millimeter-wave signal. Standard electrodeposited copper caused resistive losses to dominate the low dielectric losses of the polypropylene. Even smoother rolled copper applied to a smooth dielectric is usually intentionally roughed to make it adhere better. To minimize loss, the copper needed to be chemically treated to make it smooth and then adhered to the polypropylene with sufficient peel strength to make processing possible. A manufacturer of specialty flexible circuit boards has developed a proprietary adhesive process to adhere smooth copper to its polypropylene material. This material was used to fashion 50-ohm stripline transmission lines with a measured loss of 0.6 dB per inch.

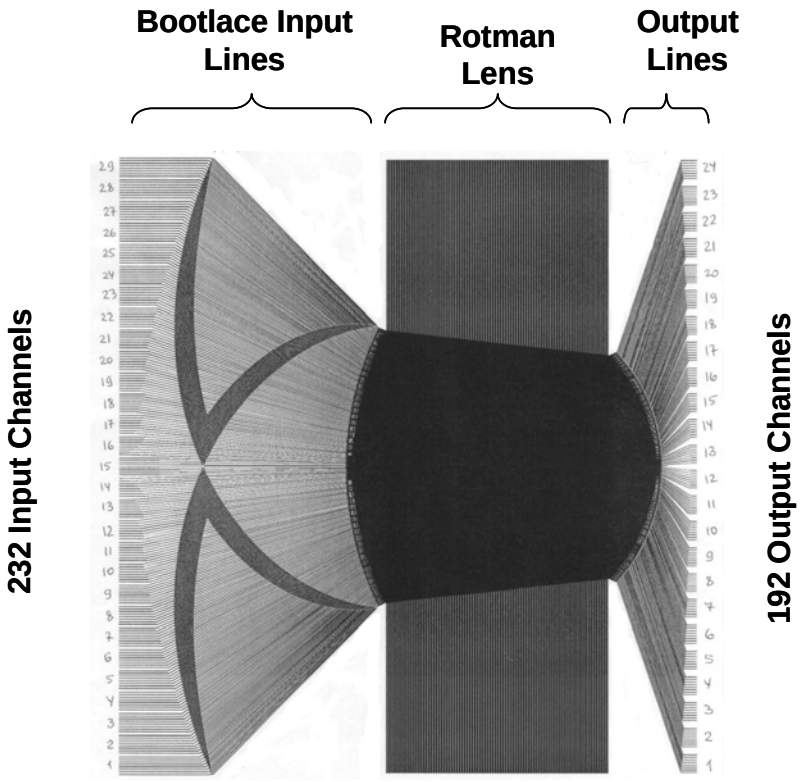

Figure 12: Phase Processor board

Stripline is composed of a transmission line suspended between an upper and lower ground plane. The dielectric material surrounds the transmission line and acts as the spacer between the ground planes. When constructing a stripline circuit, the transmission line pattern is etched on one side of a di-clad polypropylene sheet using photolithographic processes. The copper on the other side of the sheet acts as the bottom ground plane. Another sheet, with the copper removed from one side, is attached over the circuit to provide the upper dielectric and ground plane (Fig. 13). This adhesion must

provide a smooth interface free of air pockets with a sufficient strength to survive further processing. To join these two dielectric sheets, we use a heated press. The material must be heated sufficiently to join the two materials while not exceeding polypropylene's relatively low melting point of 160° C. This requires fine temperature control over the entire area of the phase processor while in the press.

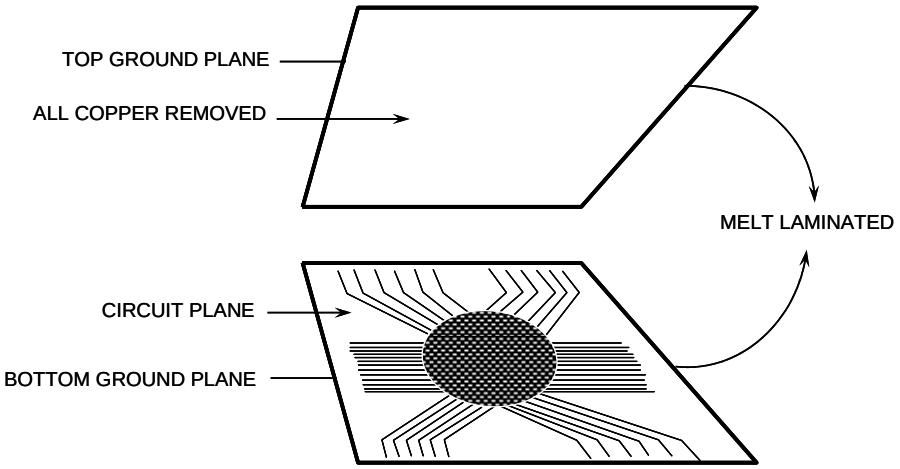

Figure 13: Processor board construction.

An additional production difficulty is involved in alignment of the two layers of material. Access to the transmission lines on the second layer is provided by holes cut in the top layer of polypropylene. As each piece of material is processed, it shrinks or grows. When the two sheets are fused together, the access holes must align with the transmission lines to better than 15 mils accuracy over 22". If the process factors are controlled to a sufficient degree, the expansion factors are repeatable and the material can be pre-compensated. Then the two pieces are kept aligned in the press through the use of specially tooled jigs. Once the pieces have been pressed together into a single sheet, the edges are trimmed and lithographically etched targets are used to locate drill holes for input and output transition fixtures.

The electrical properties of the phase processor are difficult to control at millimeter-wave frequencies. Variations in trace width, dielectric constants, or contact alignment can cause variations in system performance. The lithography tolerances for the phase processor board are not overly challenging. The narrowest linewidth is 11 mils and the minimum line separation is 9 mils, both in the splitters. The transmission lines themselves are 15 mils wide with as little as 15 mils separation. However, the long line lengths, the multiple bends, and the total distances covered on the board leave room for small errors to add up. For instance, an error in the effective impedance of a mitered corner due to over-etching will result in five separate, differently phased reflections along any processor input line. The required lithography tolerances for processor production were never quantified, but the importance of repeatability was evident. We have tested articles that were identically designed and produced and found large variations in performance quality over the frequency range. The decision to use a stripline design was made to insure a constant electrical length for the transmission lines even if the width of

the lines varied slightly. In stripline, the electric fields are contained entirely in the dielectric so variations in line width affect the effective line impedance, but not the electrical length. Another reason for the use of stripline was to control signal crosstalk and radiation. Changes in line impedance in the processor can result in radiation from the transmission lines. The ground planes in a stripline design tightly confine the electric fields, preventing radiation from traveling out of the board. Likewise, the tightly confined fields allow transmission lines to run close together without signal crosstalk. Computer EM simulations indicated that parallel transmission lines can be spaced as closely as half their width without significant crosstalk.

The stripline transmission lines in the phase processor terminate at the edges of the board. The signals are coupled from the stripline in the board to air waveguide with custom transitions. The transition path consists of WR-9 waveguide with a ridge gradually rising out of the center of the waveguide. The electric field becomes concentrated around this ridge. The ridge then contacts the stripline trace where the top ground plane has been removed to allow access. As the stripline travels into the board, the top ground plane is gradually restored to provide a smooth transition. This relatively complex transition has many opportunities for impedance mismatch and therefore reflections or radiation. A simpler transition may have been a waveguide probe transition, but this was not used for reasons of volume and geometry. A waveguide probe requires a 90-degree bend in the signal path that would have complicated the system layout. The more complex transition used by the system can perform well, however, if the board tolerances are all met. These tolerances include proper positioning of guide holes, which locate the transition with respect to the stripline traces, and the cut lines at the end of the processor board, which fits into the transition housing.

One problem that has been encountered with the input and output coupling of signals to stripline is the excitement of parallel plate TEM modes between the processor ground planes. The desired stripline mode is a quasi-TEM mode that is symmetric around the transmission line. In order to launch this mode, a symmetric field must be presented to the transmission line at the transition. The transition compresses a field from a 50 x 90 mil waveguide to a stripline transmission line with 10 mils separation from either ground plane. As such, the field is not always perfectly symmetric. The asymmetric portions of the field will excite a TEM mode between the two ground planes that is orthogonal to the stripline transmission mode (Fig. 14). While the stripline mode follows the path of the transmission line, the parallel plate TEM mode ignores the path of the transmission line and travels in a straight line across the board. This extraneous mode interferes with the desired modes, creating nulls at some frequencies, and distorts phase relationships between signals traveling in the processor lens. The interference of the parallel plate TEM mode was lessened by cutting away the ground planes in areas of the processor away from transmission lines and by adding absorber to holes drilled between transmission lines.

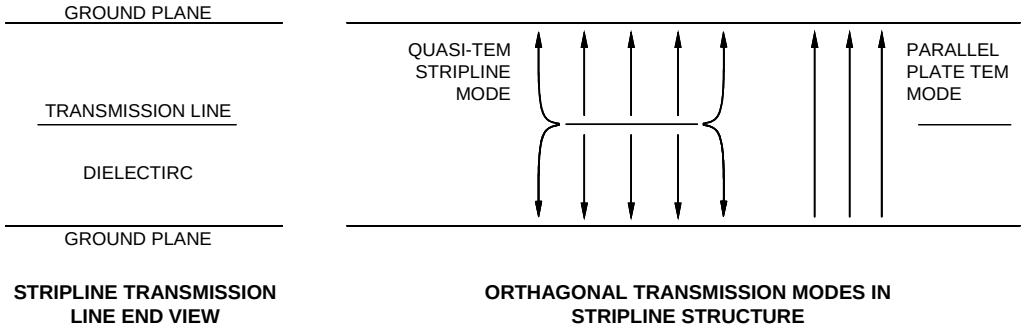

Figure 14: Modes in transmission lines

Signals traveling in the processor must make the transition from stripline transmission line to the microwave lens structure. As explained above, the stripline supports a quasi-TEM mode with impedance designed to be 50 ohms. The microwave lens area supports TEM modes between the lens area on the center conductor and the upper and lower ground planes. The lens area is where the signals are allowed to interfere and form beams at the lens outputs based upon relative phases. The lens area has lower impedance than the striplines, so a horn transition between the two modes is necessary. The horn makes a gradual impedance transition and also directs each signal input in the lens. Still, the impedance mismatch may cause reflections inside the lens. The low loss in this section of the processor means that secondary reflections can interfere with primary signals. An anti-reflective surface has been designed at the sides of the lens to lessen any stray reflections. The surface consists of transmission lines which transition from low to high impedance to gradually dissipate signals traveling along them.

Fabricated phase processor boards were tested by a network analyzer for loss and electrical length. A phase processor is designed such that a signal launched into a single output port will produce signals with linearly increasing phase along the input ports. The amount of the linear increase is proportional to the distance off center of the output launch port (Figure 15).

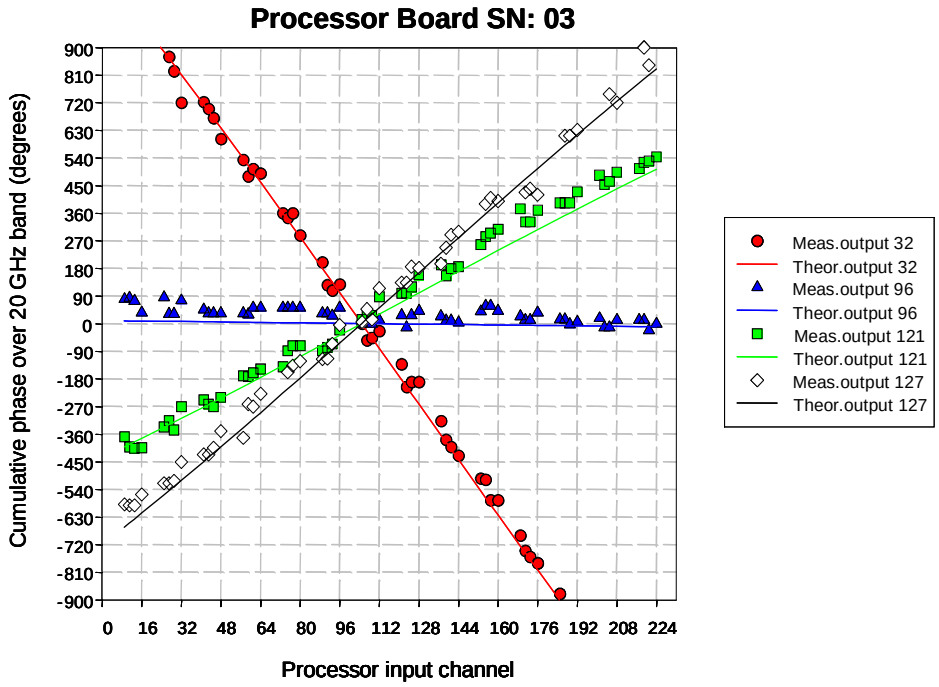

Figure 15: Sample of phase data recorded on the phase processor. The relative phases of the signals across the input channels are linear and follow the model for all four input channels tested.

MUX Chips

The MUX chips, or ROIC (Read-Out Integrated Circuits), as delivered by Indigo Systems, Santa Barbara, CA, are long narrow chips with 128 signal pins on one side of the chip and 26 control pins on the other side. The MUX chips are packaged in a 208-pin 0.5 mm pitch flat pack package by IPAC (Integrated Packaging Assembly Corporation) of San Jose, CA. IPAC uses a custom lead frame inside their package to route the wires bonded to the closely spaced chip inputs to the flat pack legs.

Pins 67-194 are input connections. The MUX chip uses differential inputs, so each pair of pins is an input channel, for a total of 64 inputs per chip. The chip also has 26 control pins, pins 14-39. The other pins on the flat pack are not connected. MUX chip control pins are as follows:

PIN	Name	Function
14	SRSYNC	Low to allow chip readout, coordinates Chip 1 with Chip 2
15	VPD	Chip power, digital logic
16	SYNC	Sync signal, cues data transfer, and accumulation cycles
17	CLOCK	Clock signal for data transfer
18	CHIP 1	High indicates Chip 1, low indicates Chip 2
19	VND	Ground, digital logic
20	VNOUT	Ground, digital output driver
21	DATA	Data line, output data from chip and control signals to chip
22	VPOUT	Chip power, digital output driver
23	VET	Vector Enabled Test to test internal logic, n/c during normal use
24	RTEST1	A/D Ramp test, n/c during normal use
25	VREFADJ	Op-amp reference adjust, n/c during normal use
26	VSHREFADJ	Sample and hold reference adjust, n/c during normal use
27	VREFRADJ	A/D ramp rate adjust, n/c during normal use
28	ATEST OD	Test A/D, n/c during normal use
29	ATESTIN EV	Test A/D, n/c during normal use
30	ITESTIN OD	Test signal input, n/c during normal use
31	ITESTIN EV	Test signal input, n/c during normal use
32	VLOWADJ	A/D ramp low voltage adjust, n/c during normal use
33	PWRADJ	Bias generator adjust, n/c during normal use
34	VPOS	Analog chip power
35	VNEG	Analog ground
36	VSUB	Substrate connection ground
37	VSIGRTN	Ground, input
38	VSUB	Substrate connection ground
39	SROUT	Signal from Chip 1 to trigger Chip 2 data readout

On each of 64 separate input channels, the MUX chips measure a differential voltage with a trans-impedance amplifier. This voltage is stored and then subtracted from the next voltage measured, with the difference being passed on the amplifier chain. This subtraction is linked to the Dicke switch of the radiometer front end, which first samples a signal from the antenna and then samples a signal from the reference load. The differencing of the two signals takes place in the MUX chip at a rate of 1.92 kHz. The signal difference is passed through a variable gain amplifier, which can be set for a gain of 0.25 to 16, and then to a 7-bit A-D converter. The output of the 7 bit A-D converter is accumulated for 63 data collection cycles, and then burst out on the 64^{th} cycle. The 63 accumulation cycles results in a 13-bit data value stored, but only the ten most significant bits are read out as data. (The MUX chip can be configured to instead output the ten least significant bits for test purposes.) The 1.92 kHz data sampling combined with the 63 accumulation cycles and one read-out cycle results in the data being burst out of the chip once every 1/30 of a second, so as to match the system display rate. The clock which reads out the data bits runs at 3.5 MHz. With two chips sequentially reading out 128

channels of 10-bit data, a full data burst requires 367μs, a fraction of the 521μs of one accumulation cycle. The data read-out is triggered by the rising edge of a long pulse on the SYNC line, and data read-out begins 82 clock cycles thereafter.

The variable gain of each MUX chip channel is set through three bits uploaded to the chip through the data line. The gain states are found in the adjoining gain table.

Gain State	Amplifier Gain
0 (0,0,0)	2
1 (0,0,1)	0.25
2 (0,1,0)	0.5
3 (0,1,1)	1
4 (1,0,0)	2
5 (1,0,1)	4
6 (1,1,0)	8
7 (1,1,1)	16

The default gain state for the MUX chips is 0, or 2x gain. To change the gain, there is an upload through the data line of 128 3-bit words. They are clocked into the chips by the 3.5 MHz clock after the data has been read out. The falling edge of a long pulse on the SYNC line indicates the chip is ready to accept input on the data line. The first bit read is a control word enable bit, which, if high, instructs the chip to read in the following 9-bit control word. The control word enables various test modes in the MUX chip and is not used during normal operation. The 11^{th} bit is a gain code enable bit, which, if high, instructs the chip to read the next 384 bits and to change the gain states of its amplifier channels accordingly. The generation of this bit stream is accomplished by the operator through the Indigo board and computer interface.

Indigo Board

The Indigo board, or read-out board, was manufactured by Indigo Systems of Santa Barbara, CA. It reads out the multiplexed 10-bit data from 192 pairs of ROICs (MUX chips), organizes the data into a 128x192 image, and passes the image to the computer BitFlow frame grabber via RS422. The Indigo board also generates the reference signal which is used to control the front-end switching and controls the MUX chips gain. Computer control of the Indigo Board is exercised over a 9-pin RS232 cable. The Indigo board communicates with the MUX chips on a 50-pin cable. There are 24 50-pin cable connectors on the Indigo board and each cable communicates with eight pairs of MUX chips, or one cassette. The signals on each cable are as follows:

Pin	Signal	Pin	Signal
1	1.92 kHz reference signal	2	Int. Test Signal Even (not used)
3	Clock 0	4	Int. Test Signal Odd (not used)
5	Sync 0	6	Power
7	Data 0	8	Power
9	Clock 1	10	Power
11	Sync 1	12	Power
13	Data 1	14	Power
15	Clock 2	16	Power
17	Sync 2	18	Power
19	Data 2	20	Analog Ground
21	Clock 3	22	Analog Ground
23	Sync 3	24	Analog Ground
25	Data 3	26	Analog Ground
27	Clock 4	28	Analog Ground
29	Sync 4	30	Analog Ground
31	Data 4	32	Analog Ground
33	Clock 5	34	Analog Ground
35	Sync 5	36	Analog Ground
37	Data 5	38	Analog Ground
39	Clock 6	40	Analog Ground
41	Sync 6	42	Analog Ground
43	Data 6	44	Digital Ground
45	Clock 7	46	Digital Ground
47	Sync 7	48	Digital Ground
49	Data 7	50	Digital Ground

The power signal is approximately eight volts and feeds the MUX chip voltage regulators on each frequency processor board. The power comes from the large 4-pin connector on the Indigo board and passes through a 10A fuse on the Indigo board before being distributed to the 50-pin sockets. Analog and digital grounds are common on the Indigo board, but are distinguished in the cable in an attempt to control noise. The clock, sync, and data signals are all TTL signals controlling the MUX chip data read-out. The level of all of these signals can be adjusted with a potentiometer on the Indigo board. If the levels are set too low, the data will not read out from all the chips and there will be black areas in the image. If the levels are set too high, there may be problems with read-out and the MUX chip gains may not be uploaded correctly. The correct setting must be determined through testing once all frequency processor cassettes have been connected to the Indigo board. The Indigo board itself is powered by a 5V signal that reaches the board on a co-axial connector in one corner of the board. This 5V power passes through a fuse and also lights a red LED as an indication that voltage has been applied (Figure 16).

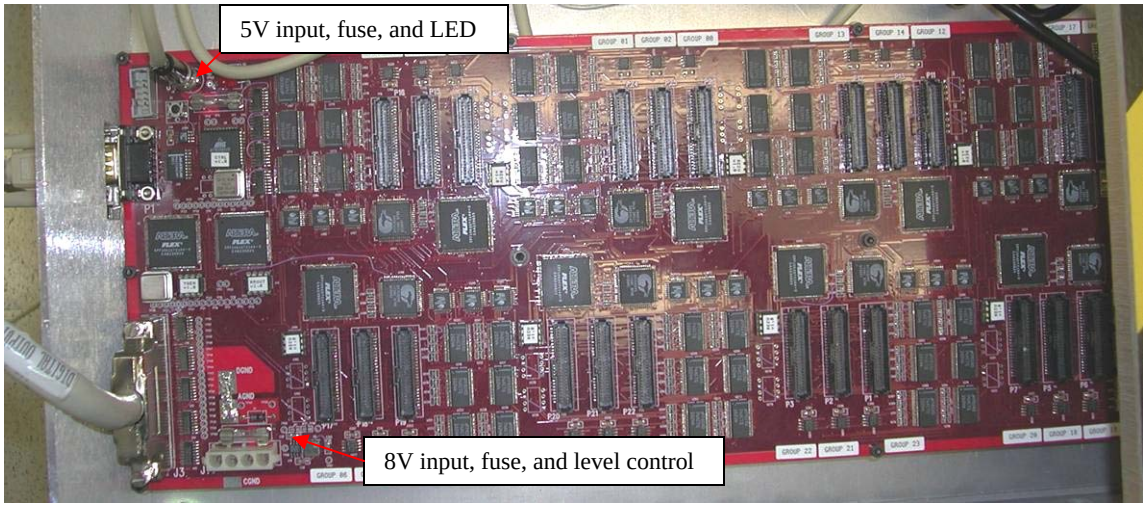

Figure 16: Indigo read-out board

Frequency Processor Board

The frequency processor sorts signals by frequency into 128 separate output ports where the signal power level is detected by a diode and converted to a voltage. Because the PMC uses a frequency scanned antenna, this sorting has the effect of sorting the signals by angle of incidence upon the antenna in the frequency scanned plane. This plane is perpendicular to the plane of the phased array. In this way, the two processors sort the energy into individual bins, each one of which represents a particular elevation and azimuth angle with respect to the antenna. The functioning of the frequency processor is conceptually similar to that of the phase processor. A single signal is sampled at various times by sending it through a splitter network with unequal path lengths. The time samples are then launched into a Rotman-like lens. The resulting beams are steered along the lens' output ports based upon the frequency of the signal. Each of the 128 output ports on the frequency processor leads to a W-band detector diode.

The frequency processor input is a waveguide probe transition which sits at the end of a WR-9 waveguide in the frequency processor transition block. The probe transition is initially created as a 50 mil length probe, the full height of the waveguide. The probe is then hand-trimmed to produce the best impedance match from the waveguide to the frequency processor stripline. The quality of match is determined by the input return loss, which is checked with a network analyzer. A return loss of 10dB or greater is considered a good match and was obtainable for most frequency processors over the band. This match was normally obtained at a probe length of 25-30 mils. The hand tuning process was necessary because the frequency processor probe lengths were not being held to the necessary 5 mil tolerances versus the alignment pins when the desired probe length was put in the initial design.

Signals travel through the frequency processor in a stripline structure created by two copper clad 10-mil polypropylene sheets surrounding a central circuit layer. This construction uses the same materials and methods as the phase processor board. The polypropylene is chosen for its low loss tangent and the ½ oz. copper cladding has a

smoothness of 15 microinches and is adhered to the polypropylene with a proprietary adhesive. The loss in a 50 ohm stripline was measured at 0.55 to 0.6 dB per inch. The low loss is necessary because of the long line lengths used in the frequency processor splitter section.

The circuit boards are created via photolithographic process to remove copper, just as standard circuit boards. The minimum linewidth and gap is four mils in the diode detector circuitry, used for high impedance matching and blocking circuits and for the gap spanned by the miniature diode. The minimum linewidth in the MMW transmission lines is eight mils, which occurs in the Wilkinson splitters. The stripline transmission line is nominally 15 mils wide with a 50 ohm characteristic impedance. A change of 1 mil in the linewidth will change the impedance by about 2 ohms. The splitter network design tries to match impedances through the mitered bends and splitters, and an error in linewidth can result in a small reflection. Even though 2 ohm error only results in about a 0.04% power reflection, the number of splits and bends in the network add up and contribute to a loss in power if impedances are not matched. The overall accuracy of feature placement on the circuit board is also important because the diode circuits must align with cutouts in the top ground plane to about 100 mils or better.

After the signal is picked up on the frequency processor transition, it travels along a 128-way stripline splitter network. Each arm of the splitter network is three wavelengths longer than the arm before it at 84 GHz. All arms of the splitter network lead to an arc of feed horns evenly spaced along a circular arc at the top of a parallel plate microwave beamforming lens. The effect of the splitter network is that the signal phase is sampled 128 times over a 4.5 ns time period, and each of these samples is combined in the lens. The total sample time of 4.5 ns implies a frequency resolution of 220 MHz is attainable with the frequency processor. At 84 GHz, each sample has the same relative phase to 2π, so the lens combines the signal samples at the central output port at the bottom of the lens. At lower frequencies, the phase lag across the lens inputs steers the beam to the output ports on one side of the lens. At higher frequencies, the beam is steered in the other direction. There are a total of 128 output ports across the bottom of the lens, corresponding to frequencies between 75.5 GHz and 93.5 GHz, separated by 140 MHz. This represents a 2x over sampling with respect to the antenna's frequency resolution.

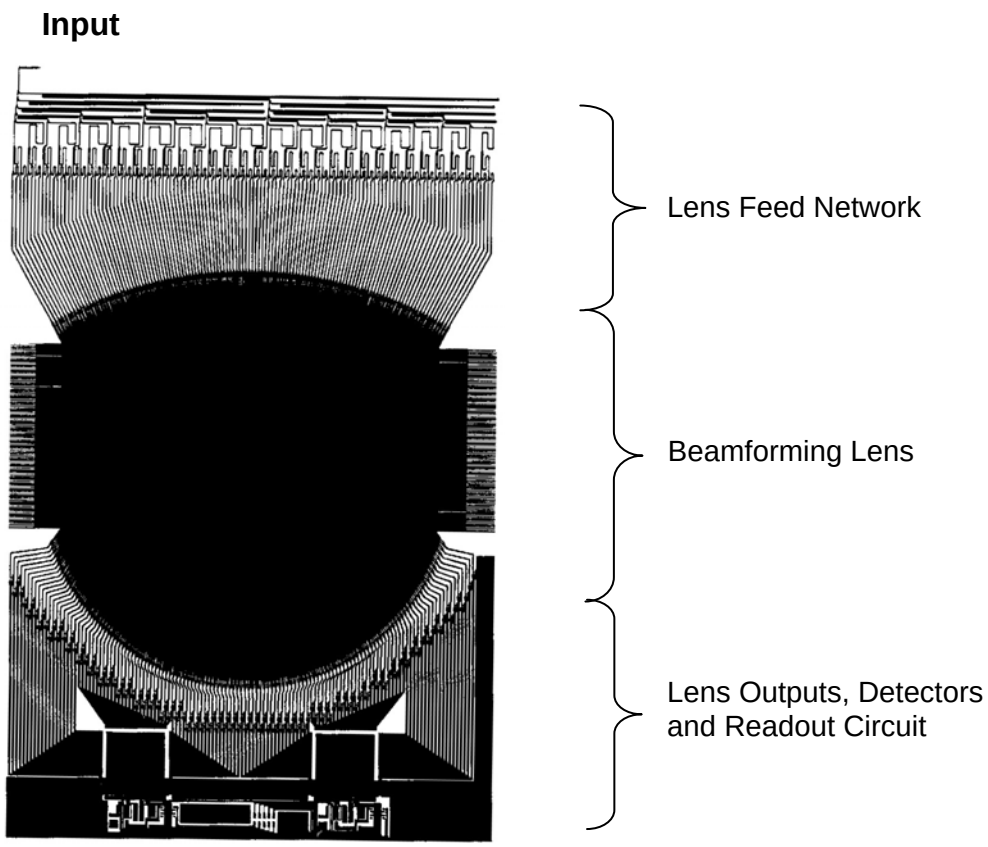

Figure 17: Stripline circuit layer of the frequency processor board.

Each output horn on the frequency processor lens transitions to a short stripline section, which feeds a diode detector circuit. The diode detector circuit consists of a transformer section to maximize coupling into the diode, tuned to the frequency of the output port, and low pass filter on a pair of high impedance DC lines leading away from either side of the diode. The diode, described below, converts the millimeter-wave energy into a voltage differential on these DC lines. The 128 voltages generated are read by a pair of ROIC (MUX) chips, as described above.

The diodes are placed on the diode detector circuits through 128 small access holes cut into the top ground plane and dielectric layer. The assembly task of placing a diode into this recess and aligning the 5 x 10 mil pads to the detector circuit proved too difficult to do automatically and was instead done by hand, using conductive epoxy for bonding. Once the diode was placed and electrically tested for DC connectivity, the cavity where the diode sits was filled with an insulating epoxy which mimicked the processor board dielectric and then covered with copper foil. This step helped concentrate the fields around the diode and raised the sensitivity of the mounted devices.

The two MUX chips and associated components are placed on the central circuit layer through two large access holes cut in the top ground plane and dielectric. The components are secured with a conductive epoxy because the low melting temperature of the polypropylene precludes the use of conventional solders. The MUX chip on the left

of the board is referred to as MUX chip 1, and it reads out its 64 voltage values before signaling MUX chip 2 to read out. The other components include a voltage regulator that converts incoming 8V to 5V. The 5V then passes through a conditioning network of bypass capacitors and in-line 11-ohm resistors before making connections to the MUX chips three power pins. All power and data connections to the frequency processor board are made though a 10-pin connector at the bottom center of the board. The 10-pin connector has the pin connections shown in figure 18, when seen end on. Note that the MUX 1 and MUX 2 connections are tied together in the flex connector.

MUX 2 SYNC	MUX 2 CLOCK	MUX 2 DATA	MUX 2 GND	MUX 2 POWER
MUX 1 POWER	MUX 1 GND	MUX 1 DATA	MUX 1 CLOCK	MUX 1 SYNC

Figure 18: 10-pin connector pin connections on frequency processor board.

Frequency processor boards were created in two varieties designated ‘A’ boards and ‘B’ boards by us. The two varieties were necessary so that the boards could nest together, face-to-face, in assembly. When viewed face-on, ‘A’ boards have the probe input at the upper left corner while ‘B’ boards have the probe input at the upper right (Figure 19). Because the boards are fed from different sides, the frequencies are steered in different directions. In ‘A’ board, the lower frequencies are steered to output ports on the left side and their power levels are read-out first by the MUX chip. In ‘B’ boards, the lower frequencies are steered to output ports on the right, so the higher frequencies have their power levels read-out first. Otherwise, the boards are functionally identical.

After assembly of all components into a frequency processor board, the board was tested for sensitivity and sidelobes. The board input was placed in a test transition and a swept signal was injected. As the signal swept from 75 to 95 GHz, the read-out from all diode detectors was logged. A print out of calculated peak sensitivity for each diode and sidelobe level was generated and stored for every board (Figure 20).

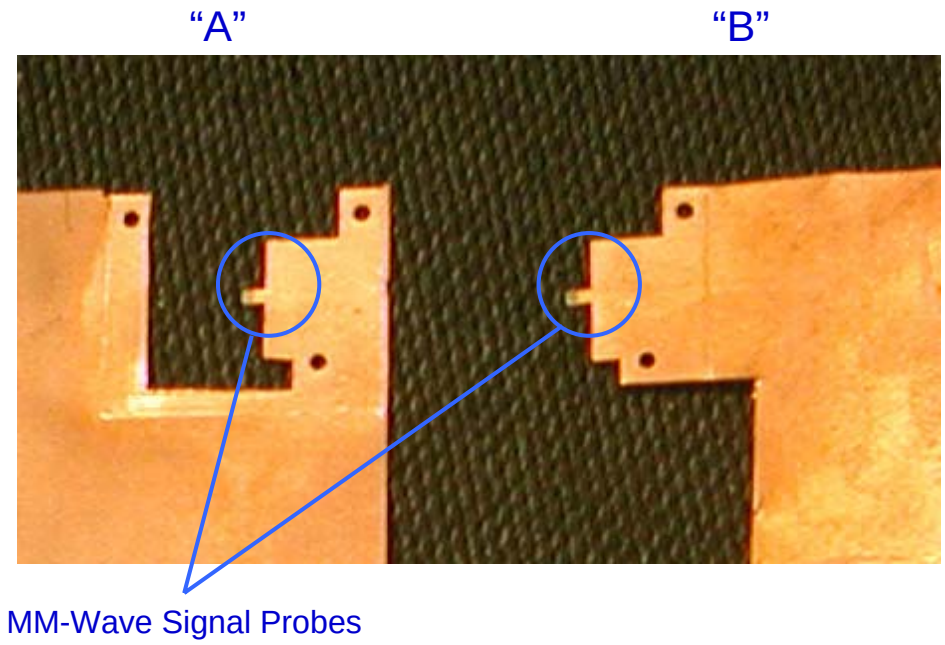

Figure 19: Input probes on 'A' and 'B' frequency processor boards.

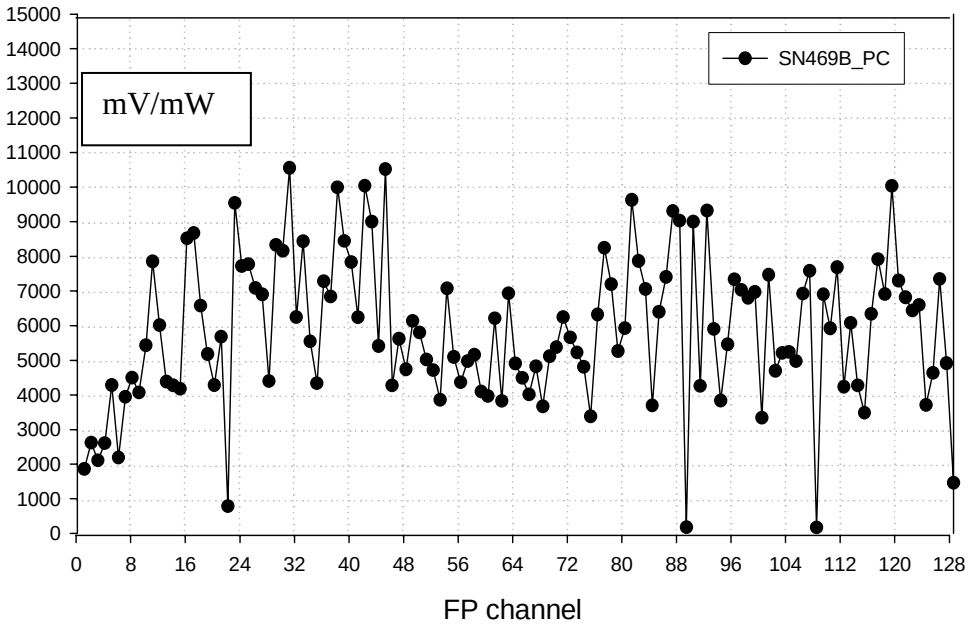

Figure 20: Sample peak sensitivity curve of frequency processor board

Diodes

The detector diodes used in the frequency processor board are Sb-heterostructure zero-bias diodes developed by HRL Laboratories, Malibu, CA. The diode operates by tunneling between an InAs layer and an AlGaSb layer which are built up vertically from a substrate. The high curvature of the I-V curve allows the diode to be used at zero-bias

as an efficient square law detector. The diodes are sensitive at W-band up to 10,000 mV/mW.

The diodes are built up using an MBE process on a wafer. When diced, each diode has a dimension of 14 mil x 19 mil with 5 mil x 10 mil contact pads (Figure 21). The diodes are hand placed into gel packs, and then assembled into the frequency processor using conductive epoxy.

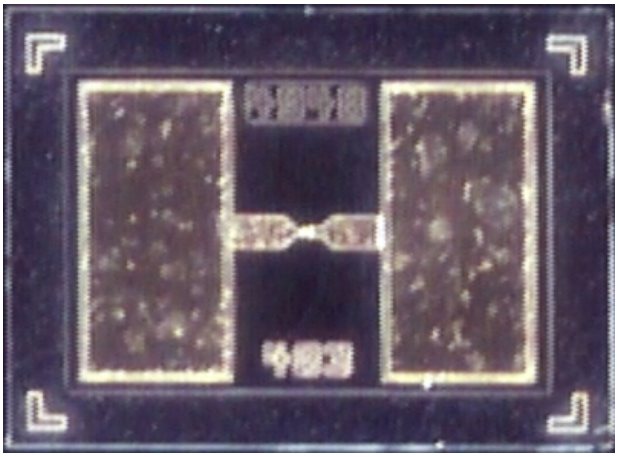

Figure 21: Picture of a detector diode. Contact pads are on either side, while the diode is in the center of the package with the leads running to it.

Transitions

The PMC has three different transitions: the antenna transition, phase processor transition, and frequency processor transition. The antenna transition is a parallel plate transition to WR-9 waveguide. The simple transition begins as a two-foot wide 36-mil air-spaced parallel plate transition clamped around the edge of the 30 mil thickness polyethylene antenna. The air gap meeting the antenna edge is only 10 mils wide. The air gap widens to 50 mils over a length of 0.6 inch, and then terminates in a row of 232 WR-9 waveguide apertures. The apertures adjoin on their narrow walls with about 10-mils of spacing. The 232 apertures are matched in 29 groups of eight to match the front-end octopak spacing.

The phase processor transitions are complex transitions from WR-9 to stripline. Eight closely spaced WR-9 air waveguides run in parallel from one end of the transition. Along a 0.5" section of this waveguide, a 10 mil wide slit along the middle of the broad walls allows for materials to be inserted into the center of each waveguide to adjust the phase length or increase attenuation. After this section, a 21 mil wide ridge rises from the opposite waveguide broad wall, slowly transitioning over 0.61" to a ridged waveguide structure and ending in a 21 mil x 25 mil flat section. When the transition is clamped around a phase processor, three dowel pins align the processor such that the flat section of the ridges comes into contact with the exposed traces in the processor.

The frequency processor transition is a block assembly with the same pattern of eight WR-9 waveguides in one side of the block. An eight mil deep probe from each frequency processor board enters the waveguide one-quarter wave before the waveguide

terminates in a back short about half way into the waveguide block. In order for the transition to accommodate the eight frequency processor boards, it is composed of nine individual plates which are built up around the boards. One of these plates is shown in figure 22. The silver area is the recess in which the input probe corner of the frequency processor board sits and the waveguide is seen from the narrow wall side as it enters the block from the top. Two dowel pin holes and four screw holes provide alignment during assembly.

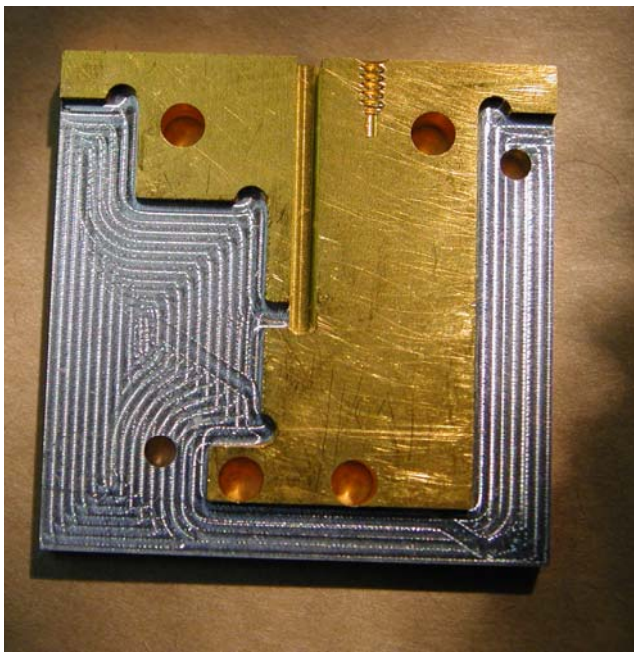

Figure 22: One plate from a frequency processor transition

System Integration

Front End

Once a fabricated phase processor board was selected for the imager based on electrical testing, its dimensions were measured. Although Sheldahl was building boards to match a mechanical drawing, the large material size combined with its dimensional instability produced phase processors of variable size. The phase processor chosen for the ARL PMC-2 was undersized in length and width. A Teklam backing plate had holes for the transitions drilled to match the length of the processor board. The twenty-nine phase processor input transitions sit side by side, so an undersized in width board must be stretched to reach these transitions. The polypropylene board can be stretched about 100 mils if the material is cut between the groups of eight transmission lines from the processor edge to the first bend. On the output side stretching was inadequate, so the twenty-four transitions were moved together slightly from their designed one-inch spacing by moving their mounting holes.

The phase processor transitions act as transitions between the waveguide input and output of the octopaks and the stripline transmission lines of the phase processor. The transitions contain segments of WR-9 waveguide running parallel to one another and are made up of top and bottom pieces so that they can be assembled around the processor board. A gap in the thin wall between waveguides as small as one mil can allow a significant level of crosstalk. This crosstalk was evident in early tests of the transitions when signals with a certain phase relationship would destructively interfere, attenuating the signal and changing the phase. Although the parts were designed to fit together seamlessly, some machining tolerances and the positioning of the screws at the ends of the transition allows a gap to open along the waveguide wall in the center of the part. In order to prevent this crosstalk, we use indium tin solder as a gasket where the waveguide wall of the bottom transition piece meets the matching grooves in the top transition piece. The solder is a special 6 mil diameter Indalloy wire from Indium Corporation of America, Clinton, NY. When the two transition pieces are joined, the soft solder compresses to fill the 10.5 mil wide groove in a strip about 3 mils thick. As the gap is generally less than 3 mils, this has the unfortunate effect of separating the transition pieces more than the design drawing, but no thinner solder wire could be prepared. If the two transition pieces are later separated, the deformed solder strip must be removed and replaced.

Installation of the phase processor board began with fastening the bottom of the input and output phase processor transitions to the Teklam backing plate. A 23" x 24" plastic backing plate of the thickness of the transitions was glued to the Teklam to act as a support for the center of the phase processor board. The phase processor was then placed over the transitions, the transitions pins locating the processor edges. The tops of the phase processor transitions first had the indium tin solder loaded into the grooves. Then the tops were pressed into place and secured with 0-80 screws, completing the phase processor transitions and holding the phase processor board in place.

At this point, the phase processor was tested on a network analyzer to confirm its electrical performance in its final assembled state. The network analyzer was used to measure loss and phase length from input ports to output ports as described in the phase processor section. Any differences from earlier test results might be due to transitions which fit differently or the indium solder gaskets. The test results for this phase processor were still good and assembly moved forward to the antenna assembly.

The antenna transition is made up of five sets of three pieces each. The five rear antenna transition pieces were attached to the Teklam plate. This piece has a small lip which locates the position of the antenna feed. Using the lip as a guide, the antenna was laid across the Teklam plate. The antenna was secured to the Teklam plate with double-sided Scotch tape and a roller to ensure antenna flatness. The tape was chosen as an adhesive because it had a fixed thickness and good resistance to sheer forces. By using a single layer aver the entire antenna area, the flatness of the Teklam plate was retained in the flexible antenna. Once the antenna was secured, the antenna transition top and front piece were added, surrounding the antenna feed. There was no conductive adhesive used

between the antenna feed and transition, as it was assumed that the physical clamping forces around the 30 mil antenna would provide good electrical contact. Although there was no evidence that this joining produced a lossier antenna feed, a conductive sealant would have ensured that no signal gaps existed. When the antenna and transition were affixed to the Teklam, the Teklam sheet was mounted to a pivoting frame and the frame placed on a rotation stage so that that the system could be pointed and tested (Figure 23).

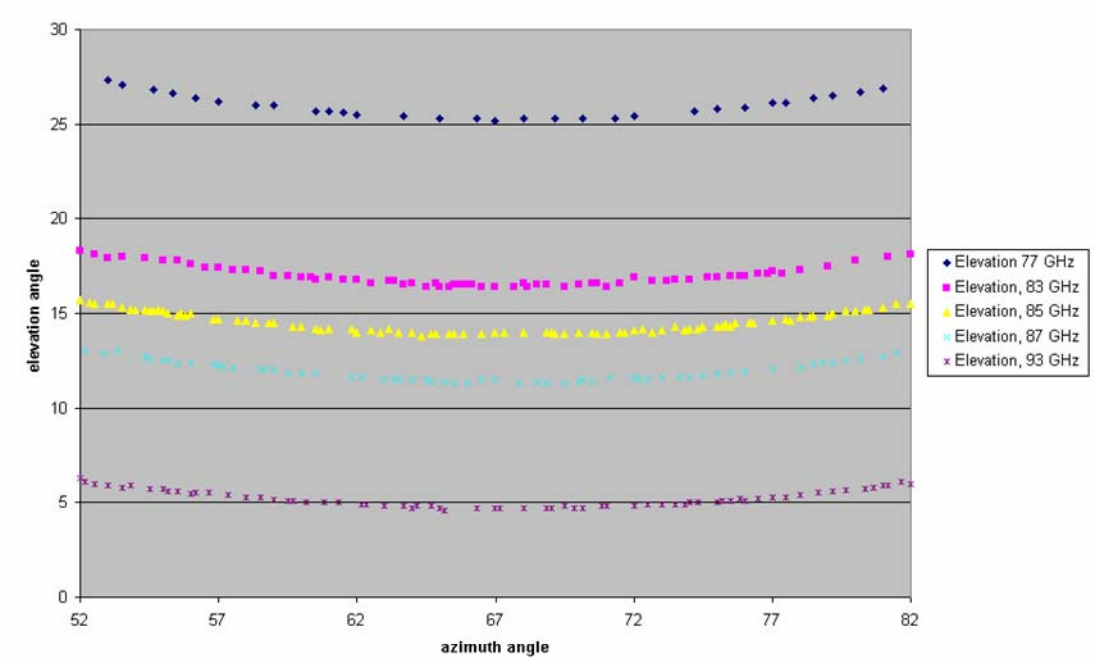

Figure 23: Antenna pointing angle at various frequencies.

The front-end octopak amplifiers were the next components to be added to the system front-end. The assembled octopak amplifier modules were tested for gain, noise figure, and phase length over their frequency range. We originally planned to select octopak amplifiers for the front-end based on noise figure, because the noise figure of the octopaks determines the temperature sensitivity of the system. After viewing the range of phase profiles of the octopaks, the front-end octopaks were selected based on how closely the phase profiles were matched. Phase profiles which varied too much over frequency could not be corrected by a simple length adjustment and would have resulted in an antenna with higher sidelobes at some frequencies. As the 29 octopaks are added to the front-end, bridging the antenna transitions and the phase processor input transitions, they form a cavity or a tunnel under the octopaks (Figure 24). The underside of the octopak amplifiers can act as a guide for evanescent energy from the octopak output to the input. Because of the high octopak gain (~55dB), it doesn't take much energy feedback to cause the system to oscillate. Microwave surface absorber material was added to the sides of the transitions and underside of the octopaks to prevent this oscillation, and additional microwave absorber foam was used to fill the space in this cavity.

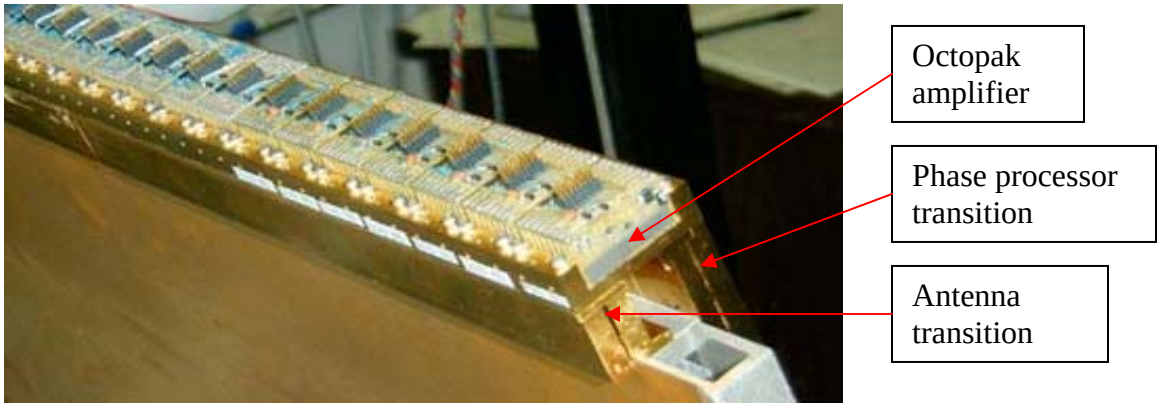

Figure 24: Octopak front-end array.

The power supplies and octopak control boards were added to the PMC frame at this point so the front end could be turned on. 16-pin ribbon cables were run from each octopak control board to the octopaks as well as some separate grounding lines. The power supplies which supply the octopak control boards with 3.3 V and +/-5 V were wired and activated. Heat sinks were added to the octopaks and a temporary set of fans were wired to cool the closely set octopak amplifier array. When the system is first turned on, it is first tested for amplifier channel operation and oscillation. Output power for the system is measured at a good phase processor output channel, as determined by the earlier processor testing. The remaining phase processor output channels are terminated with wedges of absorber material so that their output does not feed back into the antenna.

The front-end was tested by individually turning on each of the 232 amplifier channels and measuring the output power with the switch in the antenna and load positions. Power was typically in the 10 nW range for a single channel. A few channels had a higher power reading when switched to the antenna as opposed to the load, indicating channel feedback and oscillation. After trying to mechanically control the feedback, the channels were simply turned off.

System Phase Up

The 232 front-end amplifier channels of the PMC must have their electrical lengths precisely controlled in order to form antenna beams with high main beam efficiency and low sidelobe levels over the imager's field of view. The adjustment of the channel lengths is a process referred to as "phasing up the antenna". A MMW point source placed in the far field acted as a calibration standard for the antenna phase up procedure. The MMW source used was an Agilent 83558A MMW source module driven by an Agilent 83624B sweep generator placed at a distance of 100' from the antenna and imaged into the far field with a Rexolite lens. By measuring the power of the source at a phase processor output, we determine the shape of the antenna beam formed and thus the relative phase lengths of the amplifier channels.

To begin, the MMW source was set to a center band frequency and the antenna positioned to receive the signal with all front end amplifier channels switched off. Then

we selected a channel in the center of the array with a strong output signal to act as a reference. Turning on this reference channel and a second channel produces a signal at the phase processor output with a strength based on the relative phase of the two amplified signals. The relative phase is determined by the difference in electrical path length between the two channels in the imager and the angle of the antenna array to the far field source. By rotating the antenna, the relative phase of the signals changes and the signal strength rises and falls. The antenna was rotated until the signal strength reached a maximum and the rotation stage position was noted. This procedure was repeated for all the array channels, using reference channels at a suitable distance from the channel to be tested.

After generating a rough map of the relative phase differences between all the channels, the channel lengths were adjusted with strips of 10 mil thickness Duroid 5880 material from Rogers Corporation, Chandler, AZ. The material is inserted into the 0.5" long slots in the phase processor input transitions, putting them in the center of the waveguide (Figure 25). The 2.2 dielectric constant of the material slows down the signal propagation, effectively lengthening the channel, and the material ends are mitered to avoid reflections. The amount of electrical length added is set by the length of the strip inserted, with a full 0.5" strip adding about 8 ps of travel time, or about 240 degrees at a center frequency of 84.5 GHz.

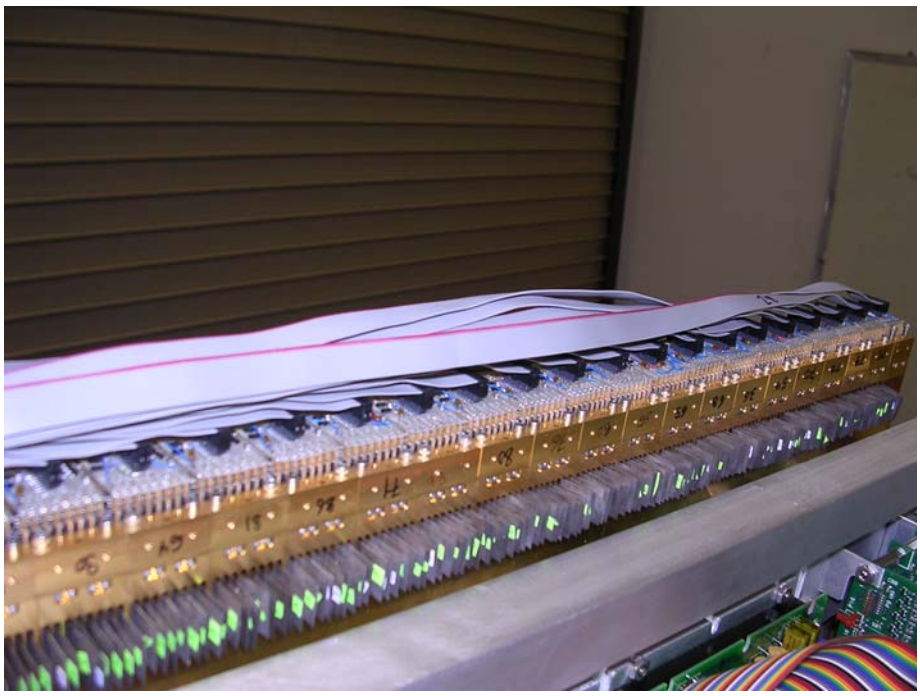

Figure 25: Duroid inserts adjust phase length in the array. The ends protruding from the transitions are later trimmed off.

The rough adjustment brought the array more closely into phase, producing a much stronger antenna beam than that of the starting state. But the adjustments were only made at the center frequency, and the antenna must be phased across the entire frequency band. The procedure described above for measuring phase length differences was repeated for

five different frequencies in the band: 79 GHz, 83 GHz, 85 GHz, 87 GHz, and 91 GHz. The necessary length adjustments calculated at each frequency were averaged together into a final adjustment. Averaging the phase adjustments is a compromise which does not produce a diffraction limited antenna beam at any one frequency, but is made necessary because of the non-linear phase behavior of the amplifiers and the fact that we only have a linear correction material. The calculated final phase adjustments for the PMC antenna are shown below in Figure 26. Only the relative phase delay between channels comes from experiment; the absolute phase delay is chosen such that as many channels as possible fall into our range of correction, 0 to 8 ps. Adjustments were made with the same Duroid 5880 strips in increments of 1 ps. When a correction outside the physically possible range was indicated, we used the maximum or minimum correction as appropriate.

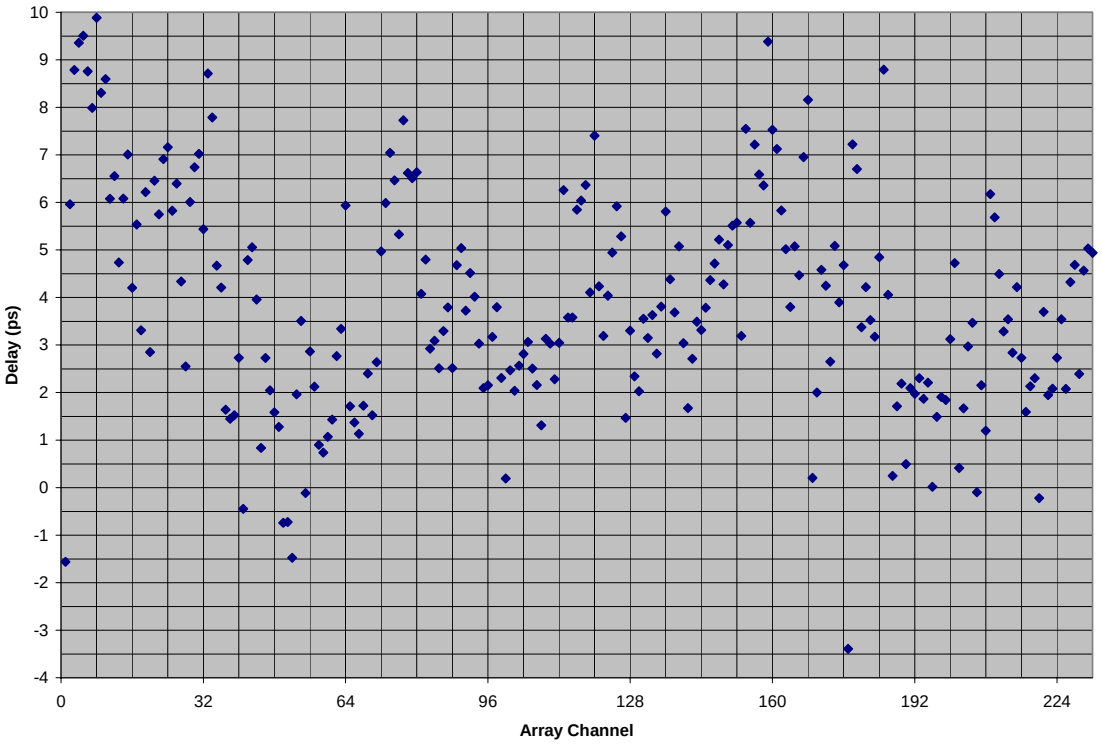

Figure 26: Final phase delays applied to antenna array

Once the phase adjustments were made, we measured antenna patterns of the system at various frequencies. Previous work had shown us that antenna patterns measured at different output ports at the same frequency were substantially the same. Some of the antenna patterns are shown below in Figures 27-29. When it was determined that the antenna patterns were acceptable, the phase shifting Duroid 5880 material was affixed in place with epoxy and the access slots in the transitions were covered with microwave absorber material.

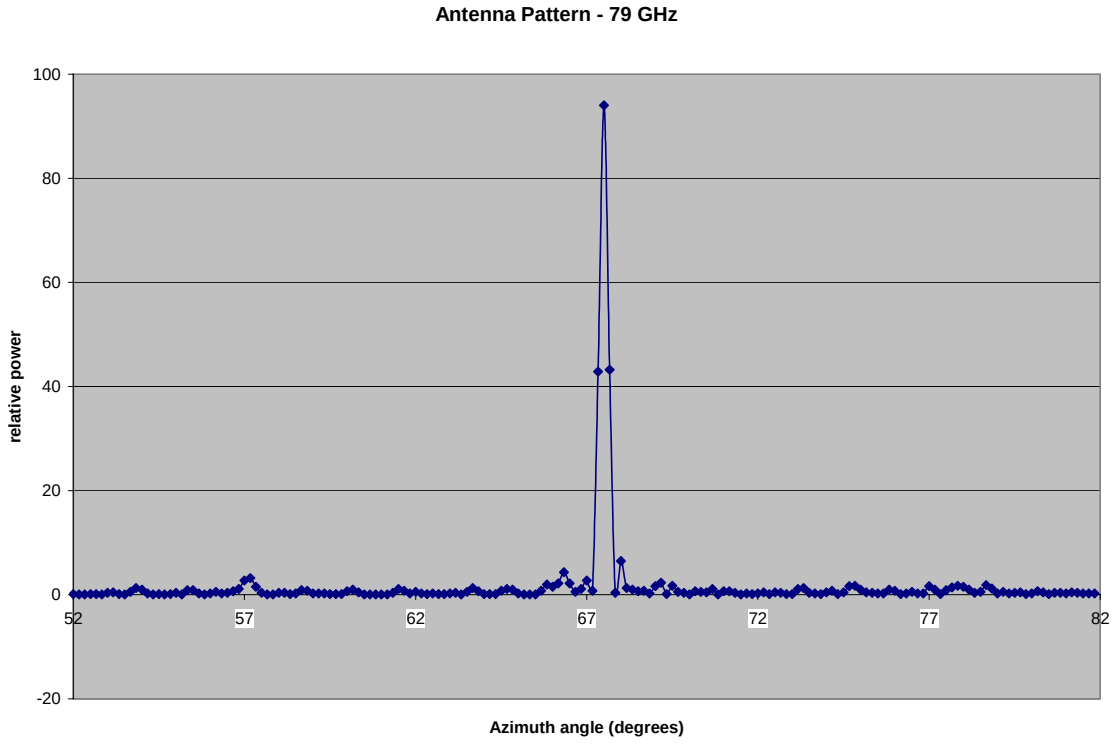

Figure 27: Azimuth antenna pattern at 79 GHz

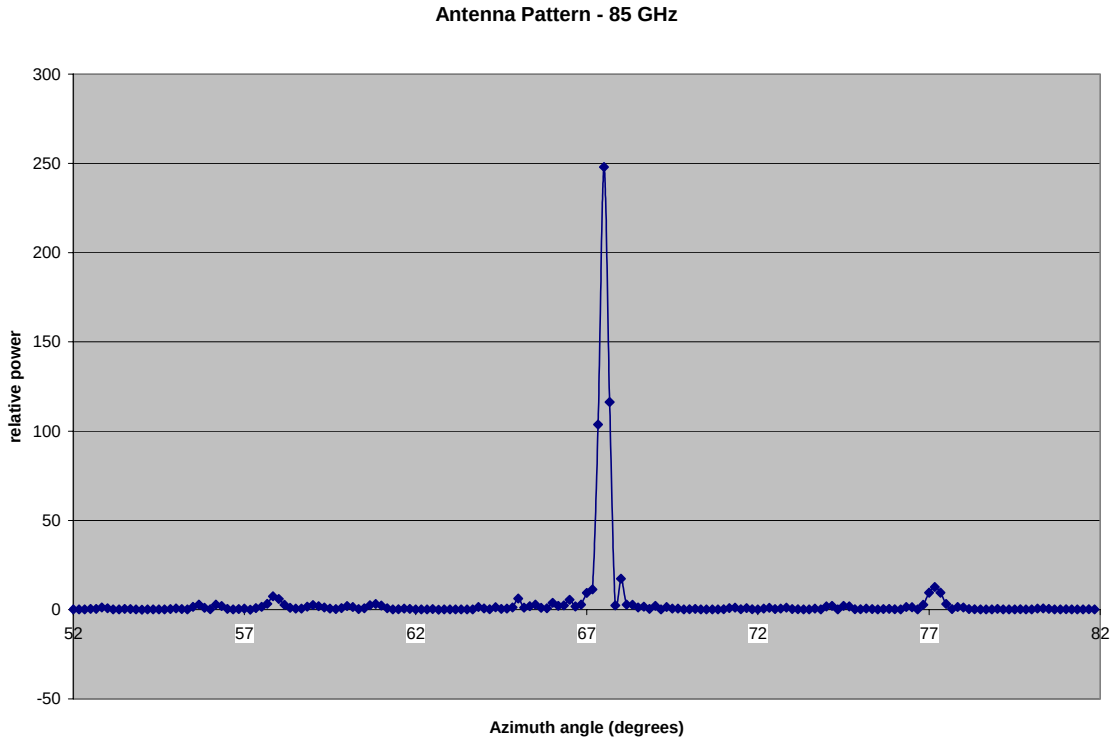

Figure 28: Azimuth antenna pattern at 85 GHz

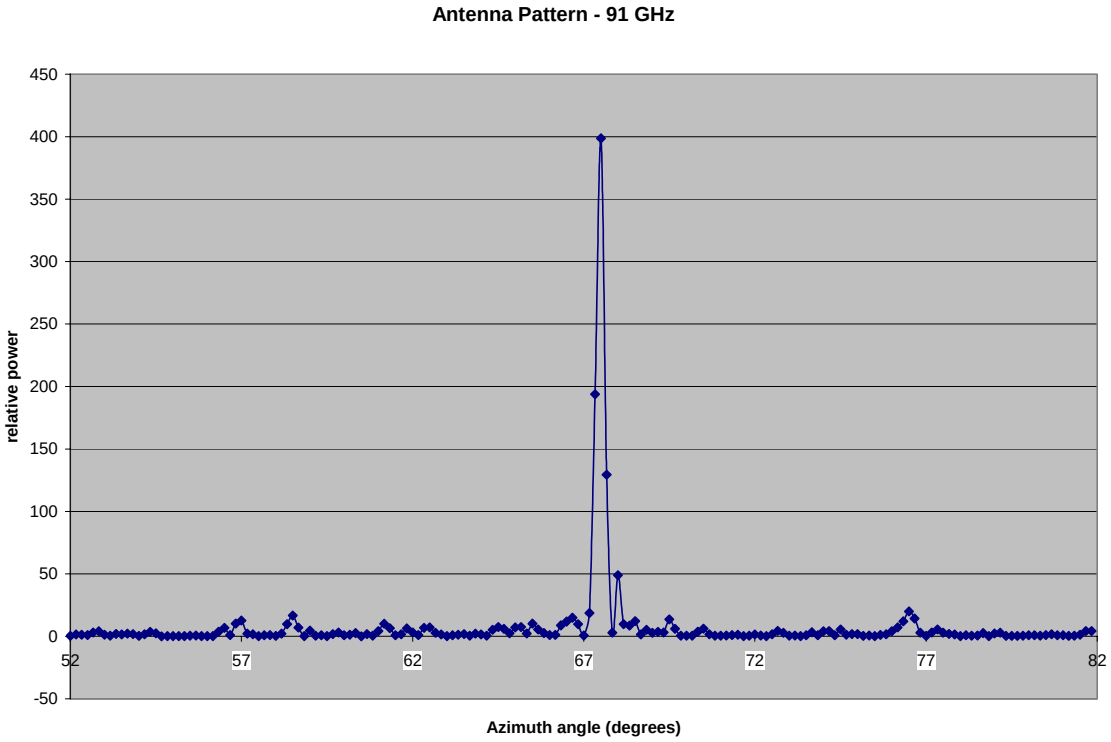

Figure 29: Azimuth antenna pattern at 91 GHz

Back-end attenuation

When the system was phased, the back-end octopaks and attenuators were added. The attenuators are necessary because the power from the phase processor output would otherwise send the back end amplifiers far into compression. The average power output of the phase processor is about -30 dBm when all front-end channels are activated. A back-end octopak power output of +1 dBm is considered optimum because it provides the maximum power difference between signal and background states, balancing lower absolute power levels against compression. With most octopak amplifier gain levels between 45-55 db, we needed 15-25 dB attenuation per channel. The original solution to adding attenuation to the system was to insert a conductive material into the waveguide channels in front of the back-end octopak amplifiers. We found that we could not accurately create 20dB of attenuation and keep the profile flat over the entire frequency range. Instead, we added absorber material inside the octopak amplifiers on the microstrip line between the second and third MMIC amplifier stages. Each octopak was retested for gain and output power after the absorber was inserted, allowing for tuning if the octopak gain curves were not within the desired range. We attempted to lower the gain of each octopak to 40-45 dB, leaving an adjustment of 5-15 dB to be made with resistive inserts.

The adjusted back-end octopaks were added to the phase processor output transitions along with the control, power, and ground wires. Each of the 192 octopak output channels were measured for total output power using a W-band diode detector to determine the amount of additional attenuation which was necessary. The attenuators

were fashioned from an 8 mil thickness Ohmega-Ply resistive-conductive laminate sourced from Ohmega Technologies, Culver City, CA. The material consists of a Nelco dielectric core laminated to a resistive nickel alloy coating to produce a 100 ohm-square resistance. The material was first cut into 0.5" long strips which could be inserted into the waveguide access slots on the phase processor transitions. Then the nickel alloy was scraped from the substrate until the desired attenuation was obtained, as measured on a network analyzer up converted to the 77-95 GHz range. The material was then inserted into the phase processor transition on the PMC-2, and the power output of the amplifier channel was re-measured. Once each output channel had been tuned to 0-2 dBm total output power, the resistive card material was fixed in place with epoxy and the access port was covered with microwave absorber material. If a back-end octopak is replaced on the PMC unit, the resistive cards for its eight channels must also be replaced. Note that although the total output level of each octopak channel was equalized, the channels can vary greatly in their output power over the frequency band. The performance over the band could not be tuned with the resistive card material, so we accepted the results. But the performance of the frequency processor cassettes would benefit greatly by having a flat power input over frequency.

Cassettes

Each cassette holds eight frequency processor boards. The eight board packaging allows one cassette to mate with one octopak and for one cassette to be mated to one 50-pin connector on the Indigo read-out board. Cassette assembly requires eight frequency processor boards (four 'A' and four 'B' boards), a cassette case bottom plate, a cassette case top, four 1" stand-offs, various spacer washers, a 50-pin to 10-pin flex-connector, and a frequency processor transition block. The flex connector is a circuit board printed on flexible material which converts the 50-pin format of the Indigo read-out board to eight 10-pin connectors in the format of the individual frequency processor boards (Figure 30). See the component description sections for pin assignments. The flexible connector allows each ten pin connector to attach securely to its frequency processor board even if the boards are different sizes. Originally, rigid boards were used for these connectors, but the variability of the frequency processor boards necessitated the switch.

The flex connector was screwed to the cassette bottom plate with a wire connecting the analog ground pins of the 50-pin connector to the cassette case. By tying the read-out chip grounds to the PMC case ground, we prevented electronic noise on the case from transferring itself to the read-out chip inputs and being read as a signal. If this connection is not made, the noise level of the cassette is greatly increased when operating in the full PMC.

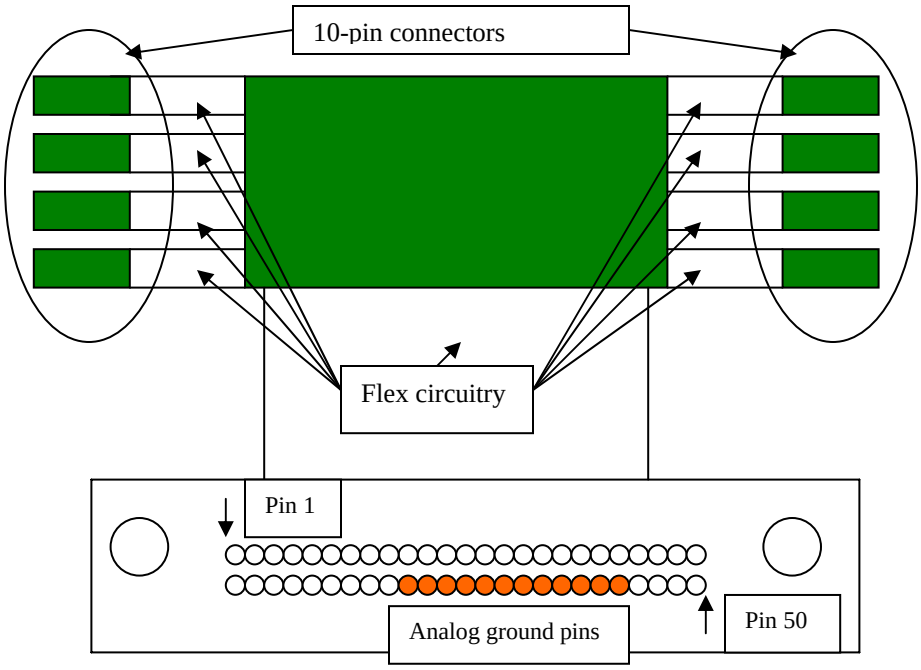

Figure 30: Drawing of flex connector detailing pin placements

Next, the four one-inch stand-off posts were screwed into the cassette bottom plate and the bottom plate of the frequency processor transition was screwed down to the cassette bottom. Now the frequency processor boards were added one at a time. The frequency processor boards fit in the cassette by having the 'A' boards face up and the 'B' boards face down. By placing them face to face, the ROICs can nest and produce a much smaller stack than if the boards were simply stacked (Figure 31).

Figure 31: Eight nested frequency processor boards viewed end on

As each board was added, it slipped over the two dowel pins in the frequency processor transition and the one-inch stand-offs. The stand-offs are there to support the frequency processor board and prevent it from putting stress on the transition. The input transition on the frequency processor board sits flush with the top face of the transition block. Then the next plate of the frequency processor transition was slipped on, trapping the frequency processor board within the transition block. The boards were alternated

between ‘A’ and ‘B’ models, with all ‘A’ boards face up and all ‘B’ boards face down. Washers were added over each stand-off as appropriate to separate the boards. The input side of each frequency processor board is separated by an equal amount to match the regular spacing of the frequency processor transition. The ROIC side of each frequency processor board has twice the input side spacing between board faces, while the back sides of the boards touch. As each board was put in place, the connection from the flex connector to the ten pin connector was made.

After all the boards were in place, the top plate of the frequency processor transition and its four screws were put in place but not tightened. In order to have a flush fit between the back-end octopak out put and the frequency processor transition block, the waveguide input face of the transition block formed by its nine component plates must be flat. The flatness of the transition face was ensured by pressing it up against a precision metal flat and then tightening the four screws which hold the transition block together. The cassette cover was then secured with eight screws and the cassette was complete.

Each assembled cassette was tested for sensitivity on a custom computer driven test set-up. The test set-up signal source was an Agilent 83558A W-band source module, was driven by an Agilent 83624B synthesized source, which was controlled by computer over an HP-IB cable. The test signal passed through an eight-way stripline splitter and through an octopak module which fed the cassette under test. The stripline splitter and octopak had been tested on a network analyzer to obtain the transfer function so it could be removed from test results. The computer swept the source through the frequency range from 75 to 95 GHz and recorded the output from each detector diode in the cassette to generate a map of the cassette sensitivity and any sidelobes. Cassettes which were found to have a non-responsive frequency processor board had the board checked and/or replaced. Cassettes which had a clear single response across the frequency band on all eight boards were installed in the PMC.

Adding Processor Cassettes

The completed cassettes were secured to the back-end octopaks with two screws through the octopak mating with the frequency processor transition. A button screw provided mechanical support for the cassette at the far end of the processor from the transition. The junction between the back-end octopak and the frequency processor cassettes was a significant source of power leakage, as the maximum power in the amplifier chain is reached here. Microwave absorber material was added to the frequency processor transition block face at the three sides of the octopak to prevent leakage. An additional piece of absorber material was also added to the cassette such that it pressed against the octopak’s fourth side when mated.

Once the cassettes were secured to the octopaks, clamps provided additional mechanical support at the two remaining corners of the cassette. The Indigo board was installed to the upper rear of the PMC frame and all power and control connections were made. Twenty-four 50-pin ribbon cables were custom cut to connect each cassette to the Indigo board. Because the Indigo board has trouble driving long cables, each ribbon cable was cut to a minimum length, and the connections maintained their order from left to right on

the Indigo board. The Indigo board 50-pin connectors do not have their addresses ordered numerically from left to right. This necessitated software remapping of all the frequency processor boards and cassettes into a coherent image.

Because the phase processor acts like a 1-D lens for the PMC system, the far left image column is created on the far right frequency processor board. The far right frequency in a cassette is read-out as board 4 of 8 because of the connections made in the 50-pin to 10-pin flex connector. And the far right cassette may be read out at cassette 9 out of 24 based on the addresses in the Indigo board. Thus, when we look at a raw read-out display, we don't have a coherent picture from left to right. A remap file is created to sort the columns back into a coherent image. The exact location of this remap file in the computer is indicated in the user's manual. The remap file is a text file listing the image columns from 0 to 191 and which of the 192 read-out column addresses is mapped to each image column. A computer routine which runs alongside the remap program is responsible for reversing the read-out order of the pixels in each 'B' frequency processor board, so that all image columns display the lowest frequencies at the top of the image.

Testing

All testing followed gain calibration of the MUX chips and a two-point software calibration of the system. The techniques for both of these procedures are described in the user's manual.

After calibration, the system was noted to experience a large amount of calibration drift. Over a period of minutes, the flat field which had been created in calibration developed a slowly shifting fixed pattern image. The amount of this calibration drift was never quantified, as it seemed to depend on system surroundings, temperature, and angle of the device. The fixed pattern noise added to images by the drift in the flat field made low contrast details difficult to discern and gave the effect of a translucent screen laid across the real image. The drift was traced to feedback in the imaging system. Power leaked from the octopak outputs was escaping the imager and being reflected back into the antenna or front-end inputs. Some front-end octopaks experienced more leakage than others, and approximately 25 of the 232 front-end channels were turned off to combat the noise problem. Additional absorber was also added around the outside of the octopaks and in the area under the front-end octopaks. This reduced but did not entirely eliminate the calibration drift. Elimination of the drift would require a mechanical redesign of the transitions to insure a full metallic seal of the waveguide interface.

Performance Test

After assembly, the PMC system underwent a series of tests to determine performance. The basic performance test is detector sensitivity. The system was pointed at the sky to create a broad cold source and then pointed at microwave absorber foam to create a broad room temperature source. The value difference of each pixel, in counts, between the two scenes indicates the signal level for a specific temperature difference, as determined by readings with a calibrated single-point radiometer. The noise of each pixel is then measured, either spatially or temporally, versus a fixed temperature scene. In a spatial

measurement, the system views a fixed temperature scene, such as microwave absorbing foam covering the antenna, and the standard deviation of pixel values over an area of the image in a single image frame is measured. In a temporal measurement, the system also views a fixed temperature scene and the standard deviation for a single pixel value over multiple frames is measured. In either case, the standard deviation of the pixels in units of temperature indicates the temperature sensitivity of the unit.

The spatial resolution of the system is a product of the phasing of the array and the beam forming quality of the phase and frequency processors. Spatial resolution was tested by imaging the edge of a high contrast target in both the vertical and horizontal directions at several places inside the field-of-view. High contrast and long integration times eliminate concerns about noise affecting the measurement. The softening of a sharp edge is the result of the edge pattern convoluted with the PMC beam pattern. The amount of that blurring indicated the angular resolution of the system, and by differentiating an image of the edge we recovered the beam pattern at that location.

Another important performance test combines antenna beam resolution and temperature resolution. By imaging targets of varying size and known temperatures, we determine the system temperature resolution for small targets. Because the antenna beam does not have all its energy in the main lobe, target temperatures are read as a combination of the actual target temperature residing in the main beam and the temperature collected from other lobes of the beam. For large targets, these other lobes may also overlap the target. For small targets, the target may not even fill the antenna's main beam. A large high contrast target, such as a metal reflector, was imaged with the PMC at a close range where it filled the field of view. Using that image temperature as a basis, the target was put at the camera's focal distance, and its temperature measured again. The ratio of the two temperatures represents the antenna beam efficiency, and the system temperature resolution is effectively scaled up by this ratio for targets of this size. The size of the target was then continuously reduced by covering areas with foam until the target occupied a single resolution cell. At this size, the apparent target temperature difference approaches the noise of the system because much of the antenna beam is no longer seeing the target. The temperature to noise ratio yields the system's sensitivity for single beam targets.

Acceptance Test

Before delivery of the PMC-2 system, a day of acceptance testing took place at Trex Enterprises in San Diego on April 1, 2004. The tests described above were performed and witnessed, as well as more basic measurements, such as antenna size and field of view. The full testing procedure and test results are appended to this document. Note that the phenomenology measurements for concealed weapons detection were briefly conducted but not formally recorded. A formal test will instead be performed at AFRL.

APPENDIX

PMC4706.PROC-1
EDITION 1 REV 4
30 MARCH 2004

PMC-2 TEST PROCEDURES

Passive Millimeter-Wave Imaging for the Detection of Concealed Weapons

Contract No. F340602-03-C-0054

Prepared for:
U.S. Air Force Research Laboratory
Rome Test Site
Rome, NY

	Name	Signature	Date
Prepared By:	Vladimir Kolinko Trex Enterprises	_____	_____
Approved By:	John G. McCoy Trex Enterprises	_____	_____
	Peter Costianes AFRL	_____	_____

TEST PROCEDURES PMC4706.PROC-1 REV 1
Passive Millimeter-Wave Imaging for the Detection of Concealed Weapons

1.0 PURPOSE

1.1 The PMC-2 Test is intended to benchmark the system's performance and verify that the PMC-2 imager is performing in general agreement with the goals set forth in Appendix 1. These procedures define the tests to be performed to satisfy this purpose.

2.0 SCOPE

2.1 The test will be performed at the contractor's facility in San Diego, CA (See CDRL A002)

The testing will include both:

- System Baseline Testing
- Phenomenology Measurements

The phenomenology measurements will include, but not be necessarily limited to, the following conditions:

- Indoor environments
- Outdoor environments
- Metallic guns
- Non-metallic guns
- Knives
- Explosives
- Edged weapons
- Frame rates varying from 30 frames per second to 1 frame per second

3.0 APPLICABLE DOCUMENTS

3.1 GOVERNMENT DOCUMENTS:

Contract F30602-03-0054

Statement of Work for Passive Millimeter-Wave Imaging for the Detection of Concealed Weapons, 21 January 2003

3.2 TREX DOCUMENTS:

User's and Maintenance Instruction Manual

3.3 DRAWINGS:

PMC2-1000 Top level and component identification drawing

4.0 MATERIALS

4.1 1 ea RF Absorber Foam Pads (24” x 24”);

4.2 1 ea Rexolite lens having 27 ft focal length (the 27 ft lens);

4.3 1 ea Rexolite lens having 15 ft focal length (the 15 ft lens);

4.4 Metal targets various sizes;

4.5 1 ea Point CW source with output power up to 0dBm and variable frequency between 75 GHz and 95 GHz;

4.6 Computer code for temperature calibration of the imager;

4.7 A set of computer codes for performing spatial and temporal statistical measurements on images (readout mean, STD and distributions for single pixel, rows, column of pixels, image areas etc.);

4.8 W-band receiver-detector with 25 dB horn antenna and sensitivity of - 60dBm or better;

4.9 Digital oscilloscope with bandwidth of at least 20 MHz and pulse duration measurement capabilities;

4.10 3ft metal ruler with 0.01 inch resolution;

4.11 A visible light video camera operating at 30 frames/sec;

5.0 EQUIPMENT

5.1 NIJ Passive MM-Wave Imager (PMC-2), operationally tested and ready for delivery except for test completion.

5.2 Test Targets

5.3 Test Weapons, including:
- Metallic guns
- Non-metallic guns
- Metallic knives
- Non-metallic knives
- Explosive surrogates

5.4 Overclothing

- Thick (jacket)
- Thin (shirt)

6.0 PRE-TEST SEQUENCE

6.1 Verify that the PMC-2 is functioning properly, using the startup and image taking procedures in the User's and Maintenance Instruction Manual

7.0 TEST SEQUENCE

7.1 MEASUREMENTS

7.1.1 BENCHMARK TESTS AND MEASUREMENTS

7.1.1.1 Field-of-View

7.1.1.1.1 Purpose

To measure and document the imager's horizontal and vertical fields-of-view (FOV). Each measurement will be made in the central section of the vertical and horizontal FOV.

7.1.1.1.2 Test Sequence

- Turn on the imager and acquire an image of the target;
- Turn the imager until target appears at the edges of its FOV.

7.1.1.1.3 Test Setup

- Mount the imager on rotation and tilt table;
- Place 100 ft lens in the imager's lens mount
- Place a flat metal target approximately 27 ft from the camera such that it reflects cold sky in the direction of the camera.

7.1.1.1.4 Test Procedure

Horizontal field-of view

- Position imager such that the image of the target is near center of imager display;
- Rotate imager horizontally to the left until only half of the target is visible at the right edge of its video image. Record azimuth angle of the imager in that position

  _____.
- Rotate imager horizontally to the right until only half of the target is visible at the left edge of its video image. Record azimuth angle of the imager in that position

_____.

- To find horizontal field of view of PMC-2 imager, compute difference between the above two angular positions of the antenna _____.
- Enter results in Data Sheet 1.

Vertical field-of view

- Position imager such that the image of the target is near center of its video image;
- Tilt imager up vertically until only half of the target is visible at the bottom edge of its video image. Record elevation angle of the antenna in that position _____.
- Tilt imager down vertically until only half of the target is visible at the upper edge of its video image. Record elevation angle of the imager in that position _____.
- To find vertical field of view of PMC-2 imager compute difference between the above two angular positions of the imager _____.
- Enter computed FOV into Data Sheet 1.

7.1.1.1.5 Data Recording and Evaluation

- Data for the field of view measurements will be recorded manually into supplied data sheet
- Calculation and results will also be recorded in Data Sheet 1.

7.1.1.2 Angular Resolution

7.1.1.2.1 Purpose

To measure and document the instrument's 3dB angular resolution. The vertical and horizontal angular resolution of PMC-2 imager will be measured near center of its field-of-view and near (within a few degrees) of the top, bottom, right, left extremes of the edges and halfway to edge and top. Total of 7 measurements.

7.1.1.2.2 Test Sequence

- Sweep antenna beam across a point CW source;
- Derive beam pattern from the PMC response data and estimate its 3dB beam width.

7.1.1.2.3 Test Setup

- Position 100 ft lens in front of the antenna;
- Position a CW frequency source with 1.5"x2" horn antenna at 100 ft distance from the antenna
- Adjust power radiated by the source such that corresponding pixel in the image is not saturated

7.1.1.2.4 Test Procedure

-Turn on the imager and warm it up for 1 hour;
- Perform calibration procedure described in User's and Maintenance Instruction Manual

Measuring horizontal beamwidth

- Set frequency of the source (e.g. 85 GHz for the beam width measurements near center of the FOV)
- Position source and turn antenna such that unsaturated image of the source appears in the desired portion of the FOV;
- Determine coordinates of the pixel that represents the image of the CW source;
- Rotate antenna horizontally 2 degrees to the left from its position;
- Perform 4 degrees left to right sweep of the antenna in 0.1 degree steps and record mean temperature reading for the selected pixel;
- Derive beam pattern by plotting pixel temperature response vs angle and estimate beamwidth at a level of –3db from the peak.
- Attach results to Data Sheet 1.

Measuring vertical beamwidth

- Set frequency of the source (e.g. 85 GHz for the beam width measurements near center of the FOV)
- Position source and turn antenna such that unsaturated image of the source appears in the desired portion of the FOV;
- Determine coordinates of the pixel that represents the image of the CW source;
- Rotate antenna vertically 2 degrees above its position;
- Perform 4 degrees top to bottom sweep of the antenna in 0.1 degree steps and record mean temperature reading for the selected pixel;
- Derive beam pattern by plotting the pixel temperature response vs angle and estimate beamwidth at a level of –3db from the peak.
- Attach results to Data Sheet 1.
-

7.1.1.2.5 Data Recording and Evaluation

- Data for the angular resolution measurements will be recorded manually into Data Sheet 1.

7.1.1.3 Thermal Sensitivity

7.1.1.3.1 Purpose

To measure and document the instrument's thermal sensitivity within its field-of-view.

7.1.1.3.2 Test Sequence

- Measure noise equivalent temperature resolution (NEdT) of the imager for a large cold target (sky);
- Estimate sensitivity degradation and NEdT for a cold target with angular size corresponding to 3dB beam width (a metal plate reflecting the sky);

7.1.1.3.3 Test Setup

- Position the 27 ft lens in front of the antenna;
- Antenna is either pointing at the sky or at the target.

7.1.1.3.4 Test Procedure

-Turn on and warm up the imager for 1 hour;
- Perform calibration procedure;

Large target NEdT measurements

- Turn antenna to view zenith (cold sky);
- Select and image area NxM pixels (minimum 5x5 pixels);
- Estimate RMS signal variations over selected area for single frame;
- Estimate RMS signal variations over selected area for several (non-averaged) frames;
- Repeat RMS measurements for different parts of the FOV (center, top, bottom, left and right sides);
- Compute beam equivalent NEdT of the system for large target by dividing the RMS values by the square root of number of pixels representing a beam (~ 4).

Beam size target NEdT measurements

-Turn antenna to point at a cold target (metal plate reflecting the sky) having angular size corresponding to 3dB antenna beamwidth ;
- Acquire single frame image of the target;
- Estimate target radiometric temperature relative to ambient _____.
- Re-acquire several times single frame images of the target and adjust antenna position for the greatest relative target temperature reading keeping same target position and pixel representing the center of the target image;
- Acquire several frames and estimate mean temperature for the pixel _____.
- Compute sensitivity degradation factor for given pixel by dividing its mean temperature value by 200 _____.
- Repeat the above beam-size target measurements by moving antenna such that the target appears in different parts of its field-of-view;
- System sensitivity for the beam size target will be calculated as a product of NEdT measured for the large target and sensitivity degradation factor corresponding to specific portion of the field of view _____.

7.1.1.3.5 Data Recording and Evaluation

- Data for thermal sensitivity measurements will be recorded manually into a data sheet and attached to Data Sheet 1.
- Results will also be entered into Data Sheet 1.

7.1.1.4 Update Rate

7.1.1.4.1 Purpose

To measure and document the instrument's image update rate.

7.1.1.4.2 Test Sequence

- Image update (video) rate is determined by system electronics and can be demonstrated by accessing frame synchronization terminals on the image acquisition (Indigo) board;
- Frame rate will be also demonstrated by imaging a moving target. A concurrent 30 frames/sec visual video recording of the moving target will be performed to compare with the PMC-2 video.

7.1.1.4.3 Test Setup

- PMC-2 imager with 100ft lens running without frame averaging;
- Outdoor setting allowing cold sky reflection from the target;
- A reflective target positioned at a height of 3 meters above the ground in the focal plane of the system.

7.1.1.4.4 Test Procedure

Testing frame rate electronically

- Get access to FRAME SYNC and GROUND terminals on the Indigo board;
- Connect oscilloscope to the terminals;
- Record and measure time period between consecutive FRAME SYNC pulses and calculate the frame rate _____.

Moving target test

- Position reflective target at 1 meter above the ground in the focal plane of the 100ft lens and a visible light camera ;
- Run visible light and PMC-2 camera without frame averaging;
- Move the target and record video sequence with both cameras for at least 1 second;
- Compare motion and appearance to validate similar frame rate.

7.1.1.4.5 Data Recording and Evaluation

-Oscilloscope snapshot of the FRAME SYNC signal will be made and signal rate measurement recorded into a Data Sheet 1 _____.

- Side by side synchronous video frames of moving target made with 30 frames/second visible light camera and PMC-2 camera will be recorded and compared. A record into a data sheet will indicate if both cameras show the same rate. Qualitative comparison _____.

7.1.1.5 Display Size

7.1.1.5.1 Purpose
To determine and document the instrument's display size (pixels x pixels)

7.1.1.5.2 Test Sequence
- Acquire PMC-2 image and determine image size in pixels

7.1.1.5.3 Test Setup
- Running PMC-2 imager;

7.1.1.5.4 Test Procedure
- Image size to be determined by importing a PMC-2 image into a software program that has an option that determines image size (e.g. Photoshop)
- Determine image size _____.

7.1.1.5.5 Data Recording and Evaluation
-Image size will be recorded into Data Sheet 1.

7.1.1.6 Antenna Size

7.1.1.6.1 Purpose
To determine and document the instrument's antenna size

7.1.1.6.2 Test Sequence
NA

7.1.1.6.3 Test Setup
- 3ft metal ruler with resolution 0.01"

7.1.1.6.4 Test Procedure
- Measure horizontal and vertical side of the slotted portion of the antenna aperture using a metal ruler with 2% accuracy H _____, V _____.
- Side lengths will be measured between corner slots in the aperture.

7.1.1.6.5 Data Recording and Evaluation
-Antenna size measurements will be recorded manually into Data Sheet 1;

7.1.1.7 Center Frequency

7.1.1.7.1 Purpose

To determine and document the instrument's center frequency

7.1.1.7.2 Test Sequence

- Position a broadband reflective target at the center of the field-of-view;
- Position a CW source in the center of FOV and determine frequency that provides maximum temperature reading of a pixel in the image that represents CW source;

7.1.1.7.3 Test Setup

- Imager with 27ft lens;
- A beam size metal target reflecting cold sky positioned in the focus of the lens;
- A CW tunable W-band source positioned next to the target at the same height;

7.1.1.7.4 Test Procedure

- Turn on, warm up and calibrate the imager;
- Acquire image of the reflective target;
- Move antenna vertically and horizontally until target image is positioned in the center of the field of view;
- Turn on CW source and tune frequency until its image appears next to the reflective target and has maximum temperature reading for given output power of the source;

7.1.1.7.5 Data Recording and Evaluation

- Record frequency corresponding to the center of the FOV per above procedure

_____

7.1.1.8 Operating Bandwidth

7.1.1.8.1 Purpose

To determine and document the instrument's operating bandwidth

7.1.1.8.2 Test Sequence

- Determine signal frequencies corresponding to the top and bottom edges of the FOV

7.1.1.8.3 Test Setup

- PMC-2 imager with 100ft lens;
- A beam size metal target reflecting cold sky positioned in the focus of the lens;
- A CW tunable W-band source positioned next to the target at the same height;

7.1.1.8.4 Test Procedure

- Turn on, warm up and calibrate the imager;
- Acquire image of the reflective target ;

Measuring the low end of the frequency band

- Move antenna until target image is positioned at the upper edge of the field of view;
- Turn on CW source and tune its frequency until its image appears next to the reflective target and has maximum temperature reading for given output power of the source;
- Record the frequency at the low end of the imager frequency band

_____

Measuring the high end of the frequency band

- Move antenna until target image is positioned at the bottom edge of the field of view;
- Turn on CW source and tune its frequency until its image appears next to the reflective target and has maximum temperature reading for given output power of the source;
- Record the frequency as the high end of the imager frequency band

_____

7.1.1.8.5 Data Recording and Evaluation

-Low and high system operating frequencies will be recorded into Data Sheet 1

7.1.1.9 Transmitted Power

7.1.1.9.1 Purpose

To determine and document the instrument's transmitted power

7.1.1.9.2 Test Sequence

- Estimate peak total mm-wave power radiated by the imager resulting from power leakage from different components;

7.1.1.9.3 Test Setup

Calibrated W-band detector-receiver with 25dB standard gain horn antenna

7.1.1.9.4 Test Procedure

- position detector-receiver at ~1 meter distance in front of the antenna and point it in the direction of the imager;
- change horn angle for maximum power reading;
- repeat the above procedure of the rear, top, left and right sides of the imager;
- record peak radiated power for each test

Front _____

Rear _____
Top _____
Left side _____
Right side _____

7.1.1.9.5 Data Recording and Evaluation
- Record peak radiated power into Data Sheet 1

7.1.1.10 System Weight

7.1.1.10.1 Purpose
To determine and document the instrument's system weight

7.1.1.10.2 Test Sequence
Measure weight of major system components and compute total system weight

7.1.1.10.3 Test Setup
-Use heavy duty scales that provides at least 2% measurement accuracy over 200 pounds weight range;

7.1.1.10.4 Test Procedure
-Weight major PMC-2 system components including :

a) Optical Head with attached antenna, octopaks, frequency processor cassettes, electronic control and interface boards, EMI/RFI shielding, cooling fans

_____

b) PC / Monitor Rack

_____

c) Rotational Stage Cart with Power Supplies

_____

d) Computed Total

_____

7.1.1.10.5 Data Recording and Evaluation
-Record individual item weights into data sheet;
-Compute and record total system weight into the Data Sheet 1.

7.1.1.11 System Noise Figure

7.1.1.11.1 Purpose
To determine and document system noise figure

7.1.1.11.2 Test Sequence
- Determine per pixel single frame NEdT for a large (sky) target;

- Estimate system noise figure from the NEdT equation;

7.1.1.11.3 Test Setup

- Position the 27 ft lens in front of the antenna;
- Antenna is either pointing at the sky or at the target.

7.1.1.11.4 Test Procedure

Perform per pixel NEdT measurements for large (sky) target within center portion of the field of view as follows;

-Turn antenna to view zenith (cold sky);
- Select and image area NxM pixels (minimum 5x5 pixels);
- Estimate RMS signal variations over selected area for single frame;
- Estimate RMS signal variations over selected area for several (non-averaged) frames;
- Repeat RMS measurements for different parts of the FOV (center, top, bottom, left and right sides);
- Record per-pixel NEdT to be equal to the measured RMS;
- Compute system noise (NF) figure from the NEdT as follows:

$$NF = 10 * \log_{10}\left(\frac{NEdT}{2 * Ta} \cdot \sqrt{\frac{BW}{FR}} \right)$$

Where Ta=290 – ambient temperature in Kelvins;
BW= $280 \cdot 10^6$ - channel bandwidth in Hz;
FR=30 - frame rate in Hz;

7.1.1.11.5 Data Recording and Evaluation

- NEdT measurements and computed NF will be recorded into Data Sheet 1.

7.1.2 PHENOMENOLOGY MEASUREMENTS

- These measurements will be performed to qualitatively evaluate visibility of various targets of interest in particular settings;
- Target visibility parameters will include its brightness contrast vs background and shape;
- Each characteristic will be estimated visually from images taken with PMC-2 and graded as GOOD, POOR or NOT VISIBLE.
- These measurements will be performed with a 15ft lens in front of the PMC-2 antenna

7.1.2.1 <u>Metallic Guns</u>

7.1.2.1.1 <u>Outdoors</u>

7.1.2.1.1.1 Purpose

To obtain outdoor phenomenology data on metallic guns using the PMC-2

7.1.2.1.1.2 Test Sequence

Take single frame and averaged video images of the target located in the chest area of the human body and evaluate its visibility under open sky conditions;

7.1.2.1.1.3 Test Setup

- Calibrated PMC-2 imager with 15 ft lens in the middle of Trex parking lot;
- Human subject carrying a metallic gun on chest positioned in the focal plane of the lens;

7.1.2.1.1.4 Test Procedure

-With subject moving slowly from side to side within focal area of the lens, record video frame sequence;
- Perform same test as above with frame rates varying between 30 FPS and 1 FPS

7.1.2.1.1.5 Data Recording and Evaluation

- Record raw and processed video data;
- Record system settings for each video sequence;
- Record target visibility evaluation based on contrast and shape into Data Sheet 2.

7.1.2.1.2 <u>Indoors</u>

7.1.2.1.2.1 Purpose

To obtain indoor phenomenology data on metallic guns using the PMC-2

7.1.2.1.2.2 Test Sequence

- Take single frame and averaged video images of the target located in the chest area of the human body and evaluate its visibility under indoors conditions;

7.1.2.1.2.3 Test Setup

- PMC-2 imager with 15 ft lens in Trex bay. Bay door(s) closed;
- Human subject carrying a metallic gun on chest positioned in the focal plane of the lens;

7.1.2.1.2.4 Test Procedure

- With subject moving slowly from side to side within focal area of the lens, record video frame sequence;
- Perform same test as above with frame rates varying between 30 FPS and 1 FPS

7.1.2.1.1.5 Data Recording and Evaluation

- Record raw and processed video data;
- Record system settings for each video sequence;
- Record target visibility evaluation based on contrast and shape into Data Sheet 2.

7.1.2.2 Non-Metallic Guns

7.1.2.2.1 Outdoors

7.1.2.2.1.1 Purpose

To obtain outdoor phenomenology data on non-metallic guns using the PMC-2

7.1.2.2.1.2 Test Sequence

Take single frame and averaged video images of the target located in the chest area of the human body and evaluate its visibility under open sky conditions;

7.1.2.2.1.3 Test Setup

- Calibrated PMC-2 imager with 15 ft lens in the middle of Trex parking lot;
- Human subject carrying a non-metallic gun on chest positioned in the focal plane of the lens;

7.1.2.2.1.4 Test Procedure

- With subject moving slowly from side to side within focal area of the lens, record video frame sequence;
- Perform same test as above with frame rates varying between 30 FPS and 1 FPS

7.1.2.2.1.5 Data Recording and Evaluation

- Record raw and processed video data;
- Record system settings for each video sequence;
- Record target visibility evaluation based on contrast and shape into Data Sheet 2.

7.1.2.1.2 Indoors

7.1.2.1.2.1 Purpose

To obtain indoor phenomenology data on non-metallic guns using the PMC-2

7.1.2.1.2.2 Test Sequence

- Take single frame and averaged video images of the target located in the chest area of the human body and evaluate its visibility under indoors conditions;

7.1.2.1.2.3 Test Setup

- PMC-2 imager with 15 ft lens in Trex bay. Bay door(s) closed;
- Human subject carrying a non-metallic gun on chest positioned in the focal plane of the lens;

7.1.2.1.2.4 Test Procedure

- With subject moving slowly from side to side within focal area of the lens, record video frame sequence;
- Perform same test as above with frame rates varying between 30 FPS and 1 FPS

7.1.2.1.1.5 Data Recording and Evaluation

- Record raw and processed video data;
- Record system settings for each video sequence;
- Record target visibility evaluation based on contrast and shape into Data Sheet 2.

7.1.2.3 Metallic Knives

7.1.2.3.1 Outdoors

7.1.2.3.1.1 Purpose

To obtain outdoor phenomenology data on metallic knives using the PMC-2

7.1.2.3.1.2 Test Sequence

Take single frame and averaged video images of the target located in the chest area of the human body and evaluate its visibility under open sky conditions;

7.1.2.3.1.3 Test Setup

- Calibrated PMC-2 imager with 15 ft lens in the middle of Trex parking lot;
- Human subject carrying a metallic knife on chest positioned in the focal plane of the lens;

7.1.2.3.1.4 Test Procedure

-With subject moving slowly from side to side within focal area of the lens, record video frame sequence;
- Perform same test as above with frame rates varying between 30 FPS and 1 FPS

7.1.2.3.1.5 Data Recording and Evaluation

- Record raw and processed video data;
- Record system settings for each video sequence;

- Record target visibility evaluation based on contrast and shape into Data Sheet 2.

7.1.2.3.2 Indoors

7.1.2.3.2.1 Purpose

To obtain indoor phenomenology data on metallic knives using the PMC-2

7.1.2.3.2.2 Test Sequence

- Take single frame and averaged video images of the target located in the chest area of the human body and evaluate its visibility under indoors conditions;

7.1.2.3.2.3 Test Setup

- PMC-2 imager with 15 ft lens in Trex bay. Bay door(s) closed;
- Human subject carrying a metallic knife on chest positioned in the focal plane of the lens;

7.1.2.3.2.4 Test Procedure

- With subject moving slowly from side to side within focal area of the lens, record video frame sequence;
- Perform same test as above with frame rates varying between 30 FPS and 1 FPS

7.1.2.3.2.5 Data Recording and Evaluation

- Record raw and processed video data;
- Record system settings for each video sequence;
- Record target visibility evaluation based on contrast and shape into Data Sheet 2.

7.1.2.4 Non-Metallic Knives

7.1.2.4.1 Outdoors

7.1.2.4.1.1 Purpose

To obtain outdoor phenomenology data on non-metallic knives using the PMC-2

7.1.2.4.1.2 Test Sequence

- Take single frame and averaged video images of the target located in the chest area of the human body and evaluate its visibility under open sky conditions;

7.1.2.4.1.3 Test Setup

- Calibrated PMC-2 imager with 15 ft lens in the middle of Trex parking lot;

- Human subject carrying a non-metallic knife on chest positioned in the focal plane of the lens;

7.1.2.4.1.4 Test Procedure
- With subject moving slowly from side to side within focal area of the lens, record video frame sequence;
- Perform same test as above with frame rates varying between 30 FPS and 1 FPS

7.1.2.4.1.5 Data Recording and Evaluation
- Record raw and processed video data;
- Record system settings for each video sequence;
- Record target visibility evaluation based on contrast and shape into Data Sheet 2.

7.1.2.4.2 Indoors

7.1.2.4.2.1 Purpose
To obtain indoor phenomenology data on non-metallic knives using the PMC-2

7.1.2.4.2.2 Test Sequence
Take single frame and averaged video images of the target located in the chest area of the human body and evaluate its visibility under indoors conditions;

7.1.2.4.2.3 Test Setup
- PMC-2 imager with 15 ft lens in Trex bay. Bay door(s) closed;
- Human subject carrying a non-metallic knife on chest positioned in the focal plane of the lens;

7.1.2.4.2.4 Test Procedure
- With subject moving slowly from side to side within focal area of the lens, record video frame sequence;
- Perform same test as above with frame rates varying between 30 FPS and 1 FPS

7.1.2.4.2.5 Data Recording and Evaluation
- Record raw and processed video data;
- Record system settings for each video sequence;
- Record target visibility evaluation based on contrast and shape into Data Sheet 2.

7.1.2.5 Explosives

7.1.2.5.1 Outdoors

7.1.2.5.1.1 Purpose

To obtain outdoor phenomenology data on explosives using the PMC-2

7.1.2.5.1.2 Test Sequence

- Take single frame and averaged video images of the target located in the chest area of the human body and evaluate its visibility under open sky conditions;

7.1.2.5.1.3 Test Setup

- Calibrated PMC-2 imager with 15 ft lens in the middle of Trex parking lot;
- Human subject carrying simulated explosive on chest positioned in the focal plane of the lens;

7.1.2.5.1.4 Test Procedure

- With subject moving slowly from side to side within focal area of the lens, record video frame sequence;
- Perform same test as above with frame rates varying between 30 FPS and 1 FPS

7.1.2.5.1.5 Data Recording and Evaluation

- Record raw and processed video data;
- Record system settings for each video sequence;
- Record target visibility evaluation based on contrast and shape into Data Sheet 2.

7.1.2.5.2 <u>Indoors</u>

7.1.2.5.2.1 Purpose

To obtain indoor phenomenology data on explosives using the PMC-2

7.1.2.5.2.2 Test Sequence

Take single frame and averaged video images of the target located in the chest area of the human body and evaluate its visibility under indoors conditions;

7.1.2.5.2.3 Test Setup

- PMC-2 imager with 15 ft lens in Trex bay. Bay door(s) closed;
- Human subject with simulated explosives on chest positioned in the focal plane of the lens;

7.1.2.5.2.4 Test Procedure

- With subject moving slowly move side to side within focal area of the lens, record video frame sequence;

- Perform same test as above with frame rates varying between 30 FPS and 1 FPS

7.1.2.5.2.5 Data Recording and Evaluation

- Record raw and processed video data;
- Record system settings for each video sequence;
- Record target visibility evaluation based on contrast and shape into Data Sheet 2.

7.2 TEST SEQUENCE:

The tests can be run in any order

7.3. DATA:

All raw PMC data to be recorded and archived

7.3 DATA REDUCTION:

All processed Images to be archived and data sheets completed for each test.

TEST PLAN PMC4664.PLN-1 REV 0
APPENDIX 1

Performance Goals for the Passive Millimeter-wave Camera (PMC-2)

Field of view	30 by 20 degrees
Angular Resolution	4 mrad
Thermal Sensitivity	2.1° K
Update Rate	30 Hz
Display Size	192 x 128 Pixels
Antenna Size	26 in x 26 in
Center Frequency	84.5 GHz
Operating Bandwidth	18 GHz
Transmitted Power	None
System Weight (sensor)	150 lb
System Noise Figure	11.3 dB

TEST PLAN PMC4664.PLN-1 REV 0
Data Sheet 1

Measured Performance of the
Passive Millimeter-wave Camera (PMC-2)

Parameter	Design Goal	Actual
Field of view	30 by 20 degrees	27.3 by 19.4
Angular Resolution	4 mrad	5.6 to 6.1 mrad
Thermal Sensitivity	2.1° K	2.6 – 8.2 K
Update Rate	30 Hz	30 Hz/15 Hz
Display Size	192 x 128 Pixels	176 x 103
Antenna Size	26 in x 26 in	23” x 24”
Center Frequency	84.5 GHz	85.3 GHz
Operating Bandwidth	18 GHz	15.2 GHz
Transmitted Power	None	< -60 dBm
System Weight (sensor)	150 lb	150 lbs.
System Noise Figure	11.3 dB	11.5 dB

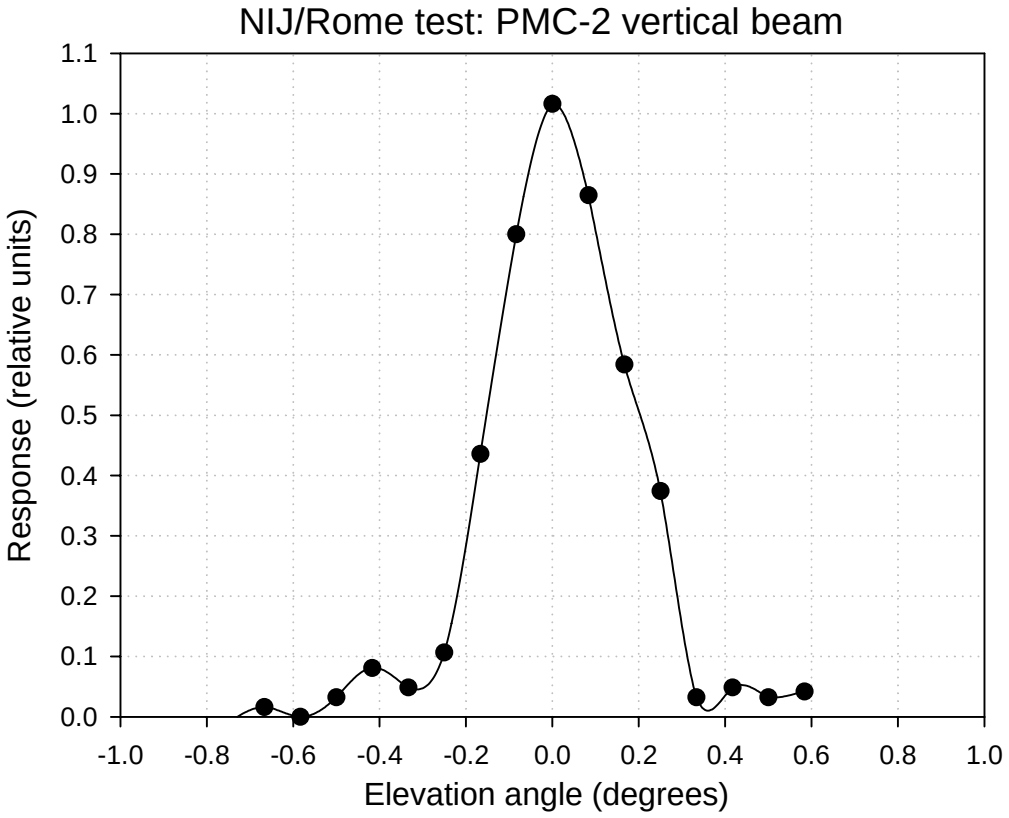
NIJ/Rome test: PMC-2 vertical beam
Response (relative units)
1.1
1.0
0.9
0.8
0.7
0.6
0.5
0.4
0.3
0.2
0.1
0.0
-1.0
-0.8
-0.6
-0.4
-0.2
0.0
0.2
0.4
0.6
0.8
1.0
Elevation angle (degrees)

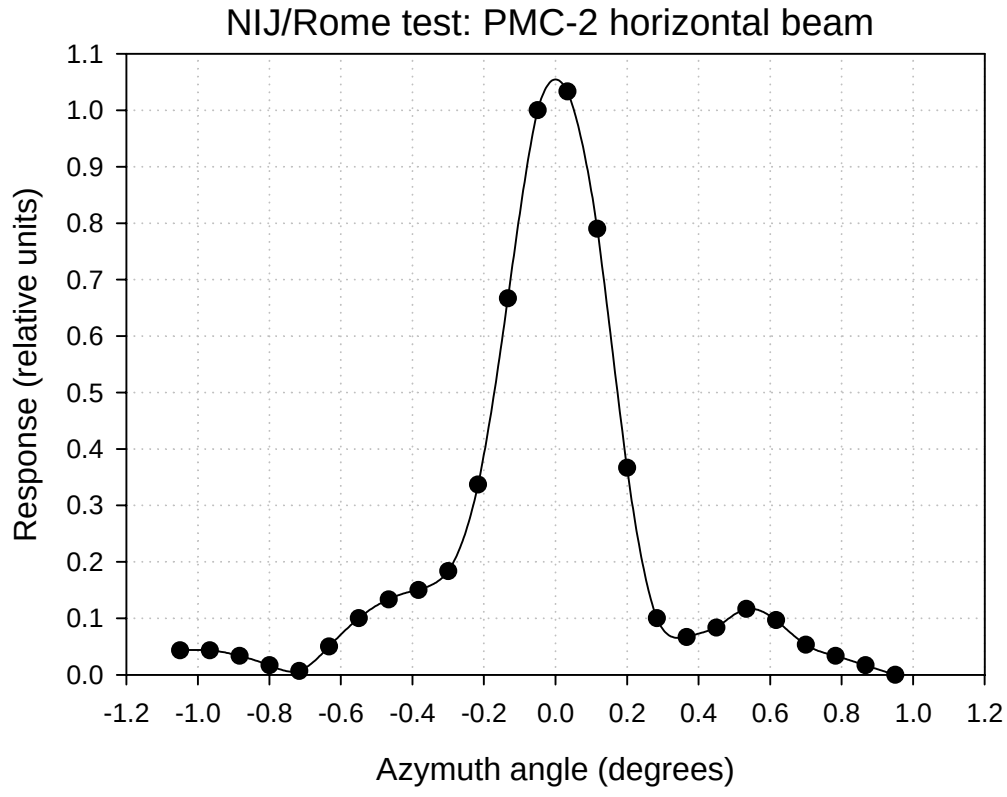
NIJ/Rome test: PMC-2 horizontal beam
Response (relative units)
1.1
1.0
0.9
0.8
0.7
0.6
0.5
0.4
0.3
0.2
0.1
0.0
-1.2
-1.0
-0.8
-0.6
-0.4
-0.2
0.0
0.2
0.4
0.6
0.8
1.0
1.2
Azymuth angle (degrees)

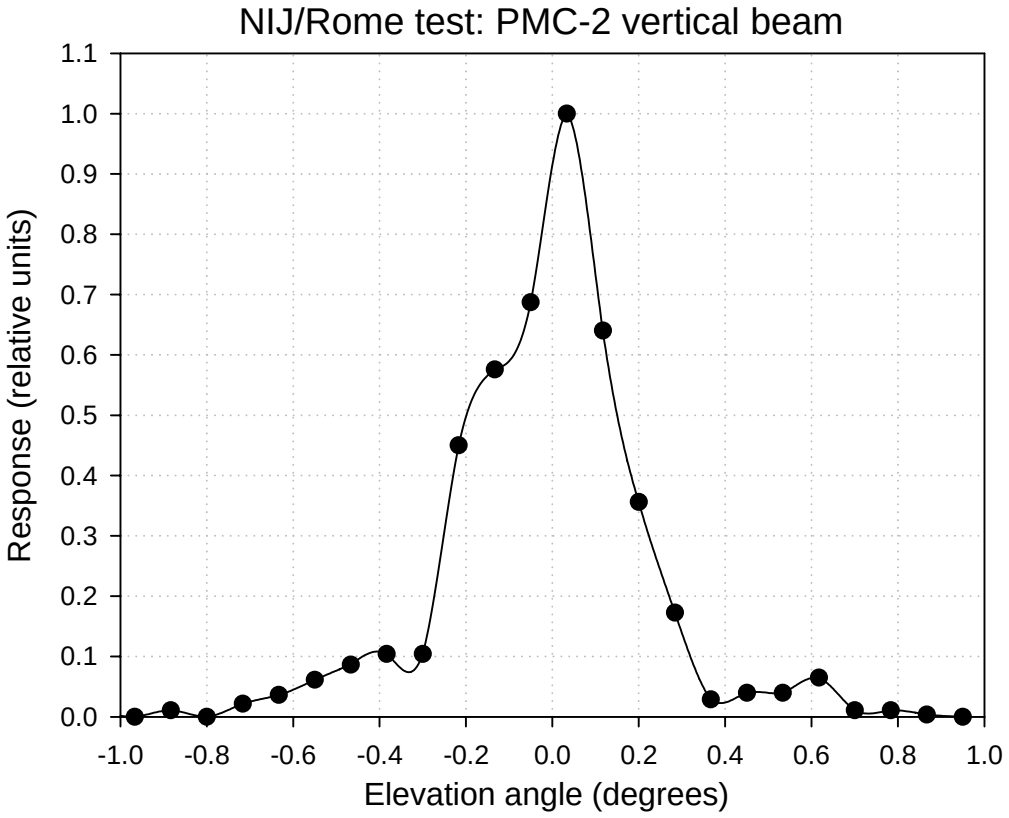
NIJ/Rome test: PMC-2 vertical beam
Response (relative units)
1.1
1.0
0.9
0.8
0.7
0.6
0.5
0.4
0.3
0.2
0.1
0.0
-1.0
-0.8
-0.6
-0.4
-0.2
0.0
0.2
0.4
0.6
0.8
1.0
Elevation angle (degrees)

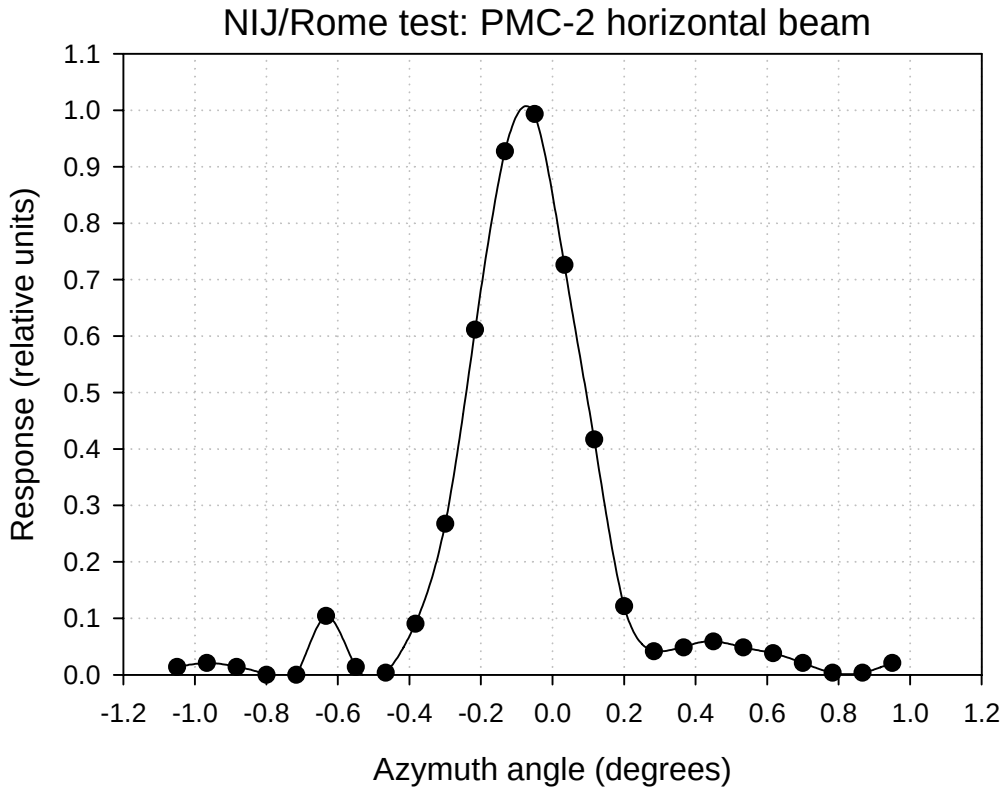
NIJ/Rome test: PMC-2 horizontal beam
Response (relative units)
1.1
1.0
0.9
0.8
0.7
0.6
0.5
0.4
0.3
0.2
0.1
0.0
-1.2
-1.0
-0.8
-0.6
-0.4
-0.2
0.0
0.2
0.4
0.6
0.8
1.0
1.2
Azymuth angle (degrees)

TEST PLAN PMC4664.PLN-1 REV 0
Data Sheet 2

Measured Performance of the
Passive Millimeter-wave Camera (PMC-2)

Parameter	Test Evaluation and Comments
Metal Gun (Outdoors)	_____
Metal Gun (Indoors)	_____
Non-Metal Gun (Outdoors)	_____
Non-Metal Gun (Indoors)	_____
Metal Knife (Outdoors)	_____
Metal Knife (Indoors)	_____
Non-Metal Knife (Outdoors)	_____
Non-Metal Knife (Indoors)	_____
Explosives (Outdoors)	_____
Explosives (Indoors)	_____